

From Calcium Interaction to Calcium Electrochemical Detection by $[(C_5H_5)Fe(C_5H_4COCH=CHC_6H_4NEt_2)]$ and Its Two Novel Structurally Characterized Derivatives

Jérôme Maynadié,[†] Béatrice Delavaux-Nicot,^{*†} Dominique Lavabre,[‡] Bruno Donnadieu,[†] Jean-Claude Daran,[†] and Alix Sournia-Saquet[†]

Laboratoire de Chimie de Coordination du CNRS, UPR 8241, 205, route de Narbonne, F-31077, Toulouse Cedex 04, France, and Laboratoire des Interactions Moléculaires et Réactivité Chimique et Photochimique, UMR 5623 du CNRS, Université Paul Sabatier, 118 route de Narbonne, F-31062, Toulouse Cedex, France

Received May 28, 2003

$[(C_5H_5)Fe(C_5H_4COCH=CHC_6H_4NEt_2)]$ (**1**) has been electrochemically evaluated toward different cations in solution. Calcium sensing by this compound and its two new derivatives $[(C_5H_5)Fe(C_5H_4CO(CH=CH)_2C_6H_4NMe_2)]$ (**2**) and $[(C_5H_5)Fe(C_5H_4CH=CHCOCH=CHC_6H_4NEt_2)]$ (**3**) that exhibit a conjugated link between the ferrocene unit and the nitrogen atom has been thoroughly examined. Compounds **2** and **3** have been structurally characterized by single-crystal X-ray diffraction studies. The three related protonated species $[1H][BF_4]$ (**4**), $[2H][BF_4]$ (**5**), and $[3H][BF_4]$ (**6**) have been isolated in a good yield. NMR experiments clearly established that calcium interaction occurs in the vicinity of the carbonyl group, and mass spectrometry studies confirmed that this interaction, which involves several ligand– Ca^{2+} adducts, is complex. A combination of electrochemical and NMR experiments highlighted an original salt influence on the electrochemical calcium sensing result.

Introduction

A plethora of redox-active or fluorescent receptors have been designed for ion recognition in solution and have proved the usefulness of electrochemistry and fluorescence in chemistry, biology, and medicine.¹ However, despite the development of these two types of sensors, few examples of fluorescent ferrocenyl ion sensors have been described in the literature.² These latter systems, which contain both types

of signaling units (electroactive and fluorescent), could be the keystone of new families of ion chemosensors that can either be able to sense different guests or display two or more macroscopic observable events upon addition of a certain analyte.^{2c,3} The fabrication of these systems and their integration into different supports (e.g., matrixes: electronically conducting polymeric supports, optical fibers, etc.) will probably lead to novel prototype molecular sensory devices of commercial usage.^{2a,4} As part of our research program aimed at the design of innovative sensors, we have recently investigated the synthesis of electroactive receptors which combine ferrocenyl units and a purely organic fluorescent ion sensor subunit containing an R-amino complexing moiety ($-COCH=CHC_6H_4-pR$, R = NEt_2 or aza-15-crown-5). We have established that new electroactive and efficient fluo-

* Author to whom correspondence should be addressed. E-mail: delavaux@lcc-toulouse.fr. Fax: (33) 5 61 55 30 03.

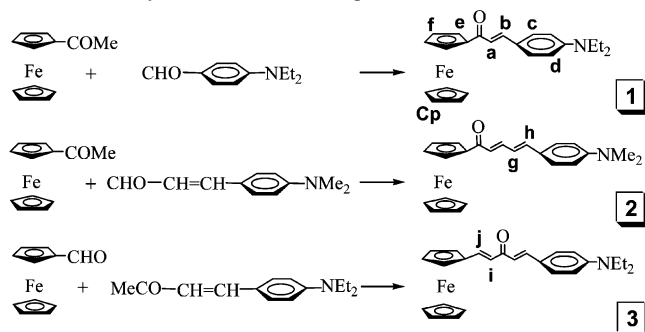
[†] Laboratoire de Chimie de Coordination du CNRS.

[‡] Laboratoire des Interactions Moléculaires et Réactivité Chimique et Photochimique.

(1) For examples in electrochemistry: (a) Beer, P. D. *Adv. Inorg. Chem.* **1992**, 39, 79. (b) Beer, P. D.; Cadman J. *Coord. Chem. Rev.* **2000**, 205, 131. (c) Medina, J. C.; Goodnow, T. T.; Rojas, M. T.; Atwood, J. L.; Lynn, B. C.; Kaifer, A. E.; Gokel, G. W. *J. Am. Chem. Soc.* **1992**, 114, 10583. (d) Delavaux-Nicot, B.; Mathieu, R.; de Montauzon, D.; Lavigne, G.; Majoral, J.-P. *Inorg. Chem.* **1994**, 33, 434. (e) Delavaux-Nicot, B.; Bigeard, A.; Bousseksou, A.; Donnadieu, B.; Commenges, G. *Inorg. Chem.* **1997**, 36, 4789 and references therein. For examples in fluorescence: (f) Prasanna de Silva, A.; Gunaratne, H. Q. N.; Gunnlaugsson, T.; Huxley, A. J. M.; McCoy, C. P.; Rademacher, J. T.; Rice, T. E. *Chem. Rev.* **1997**, 97, 1515. (g) Czarnik, A. *Fluorescent Chemosensors for Ion and Molecule Recognition*; ACS Symposium Series 538; American Chemical Society, Washington, DC, 1993. (h) Tsien, R. Y. In *Methods in Cell Biology*; Taylor, D., Wang, Y.-L., Eds.; Academic Press: London, 1989, 30, 127.

(2) (a) Beer, P. D.; Szemes, F.; Balzani, V.; Salà, C. M.; Drew, M. G. B.; Dent, S. W.; Maestri, M. *J. Am. Chem. Soc.* **1997**, 119, 11864. (b) Delavaux-Nicot, B.; Fery-Forgues, S. *Eur. J. Inorg. Chem.* **1999**, 1821. (c) Fery-Forgues, S.; Delavaux-Nicot, B. *J. Photochem. Photobiol., A* **2000**, 132, 137. (3) (a) Sancenon, F.; Benito, A.; Hernandez, F. J.; Lloris, J. M.; Martinez-Manez, R.; Pardo, T.; Soto, R. *Eur. J. Inorg. Chem.* **2002**, 866. (b) Gan, J.; Tian, H.; Wang, Z.; Chen, K.; Hill, J.; Lane, P. A.; Rahn, M. D.; Fox, A. M.; Bradley, D. D. C. *J. Organomet. Chem.* **2002**, 645, 168. (4) Maynadié, J.; Delavaux-Nicot, B.; Fery-Forgues, S.; Lavabre, D.; Mathieu, R. *Inorg. Chem.* **2002**, 41, 5002.

Scheme 1. Synthetic Route for Compounds 1, 2, and 3



Reagents and conditions: 1:1 ethanol, NaOH 5 equiv., 20° C.

resent species which contain only ferrocene as a metallic moiety could be obtained,^{2b} and that one of these compounds [$[\text{Fe}(\text{C}_5\text{H}_4\text{COCH}=\text{CHC}_6\text{H}_4\text{NEt}_2)_2]$] behaves as a new type of multiresponsive calcium-sensing device.⁴

In contrast to its disubstituted counterpart, compound [$(\text{C}_5\text{H}_5)\text{Fe}(\text{C}_5\text{H}_4\text{COCH}=\text{CHC}_6\text{H}_4\text{NEt}_2)$] (**1**) is not fluorescent in CH_3CN . But, preliminary results have shown that interposition of the conjugated $-\text{COCH}=\text{CHC}_6\text{H}_4-$ spacer between the ferrocene unit and the NEt_2 ionophore in this compound could allow an electronic communication through the link. This property is of real importance and suggested that molecules containing the fluorescent organic fragment could be electrochemical sensors. Furthermore, an electronic communication through the link has also been demonstrated for ferrocenyl systems incorporating a $-\text{CH}=\text{CHC}_6\text{H}_4-$ spacer.⁵ Other teams have also studied related compounds (analogues of **1**) incorporating a CO function directly linked to a ferrocenyl moiety,⁶ however none of these compounds was evaluated toward electrochemical sensing. Recently, such related ferrocenyl chalcone systems attracted a revival of interest and were tested toward antimalarial activity⁷ or as potential anticancer drugs.⁸

Here we report on the synthesis, characterization, reactivity, and electrochemical properties of compound [$(\text{C}_5\text{H}_5)\text{Fe}(\text{C}_5\text{H}_4\text{COCH}=\text{CHC}_6\text{H}_4\text{NEt}_2)$] **1** and of its two new mono-substituted derivatives **2** and **3** containing an olefinic fragment after and before the carbonyl group (Scheme 1). Compounds **2** and **3** were synthesized to get a better understanding of the factors which could influence the electronic communication in this family and consequently the cation detection. We were particularly interested in understanding and quantifying the interaction processes which occur with the Ca^{2+} cation and the pathway between interaction and signaling.

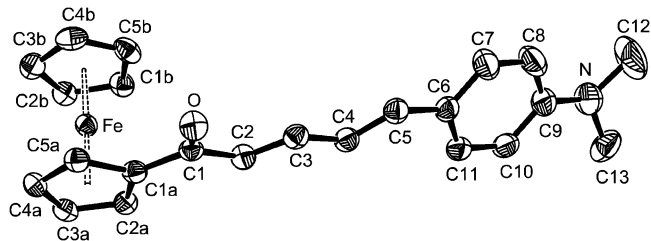


Figure 1. Molecular view of the structure of compound **2** (ORTEP 3) with 50% thermal ellipsoids.

Results and Discussion

1. Synthesis and Characterization of Ligands 1, 2, and 3. As for compound **1**,^{2b} compounds **2** and **3** were obtained in good isolated yield (72–82%) by reaction of acetyl ferrocene and ferrocene carboxaldehyde with the appropriate organic reactants in basic medium.

New experimental conditions allowed a significant improvement in the isolated yield of **1** when compared to our precedent published procedure.^{2b} The reverse aldol condensation reaction could be suppressed in absence of water. The IR spectra of molecules **1**, **2**, and **3** exhibit vibrations at 1647, 1646, and 1642 cm^{-1} in CH_3CN , respectively, assigned to stretching CO vibrations.^{9a–c} This low value is due to the conjugation of the CO group with the π system ($-\text{CH}=\text{CHC}_6\text{H}_4-$) in the molecule.^{2b,9d} These vibrational assignments are presently under theoretical investigation.¹⁰

The structure of these molecules was first deduced from spectroscopic data. 2D NMR experiments (HMQC and NOESY) clearly verified the assignments. Elemental analyses and mass spectra are also in agreement with the proposed formula (see Experimental Section). In the ^1H NMR, for compound **2**, the olefinic protons Ha and Hb in α and β position toward the CO function presented an upfield shift when compared to those of **1** and **3** (+ 0.20 ppm). In compound **3**, as for the symmetrical related compound [$(\text{C}_5\text{H}_5)\text{Fe}(\text{C}_5\text{H}_4\text{CH}=\text{CHCOCH}=\text{CHC}_5\text{H}_4)\text{Fe}(\text{C}_5\text{H}_5)$]^{9a} and the [Fe–Cr] compound [$(\text{C}_5\text{H}_5)\text{Fe}(\text{C}_5\text{H}_4\text{CH}=\text{CHCOCH}=\text{CHC}_6\text{H}_5\text{Cr}(\text{CO})_3)$]^{9b} very similar shifts are observed for the Ha and Hi protons in α position to the CO function and for the Hb and Hj protons in β position.

Crystal of **2** and **3** suitable for X-ray structural analysis were obtained by slow recrystallization in CH_3CN . Perspective views of the molecules are shown in Figures 1 and 2, respectively. Crystallographic data for compounds **2** and **3** are provided in Table 1. Selected bond lengths and bond angles are listed in Table 2. In both compounds the Cp rings are nearly eclipsed with twist angles of 3° and 9.3° for **2** and **3**, respectively (see S10 and S11 in the Supporting Information). The bond lengths within the ferrocenyl

(5) Andrews, M. P.; Blackburn, C.; McAleer, J. F.; Patel, V. D. *J. Chem. Soc., Chem. Commun.* **1987**, 1122.

(6) For example: (a) Nagy, A. G.; Toma, S. *J. Organomet. Chem.* **1984**, 266, 257. (b) Nagy, A. G. *J. Org. Chem.* **1984**, 291, 335. Dubosc, J. P. C. G. U.S. Patent 3,335,008, 1967. (c) Nesmeyanov, A. N.; Shulp'in, G. B.; Rybin, L. V.; Gubenko, N. T.; Rybinskaya, M. I.; Petrovskii, P. V.; Robas, V. I. *Zh. Obshch. Khim. (J. Gen. Chem. USSR)* **1974**, 44, 1994. (d) Toma, S.; Perjessy, A. *Chem. Zvesti* **1969**, 23, 343. (e) Boichard, J.; Monin, J. P.; Tirouflet, J. *Bull. Soc. Chim. Fr.* **1963**, 4, 851.

(7) Wu, X.; Wilairat, P.; Go, M.-L. *Biorg. Med. Chem. Lett.* **2002**, 12, 2299.

(8) Ferle-Vidovic, A.; Poljak-Blazi, M.; Rapic, V.; Skare, D. *Cancer Biother. Radiopharm.* **2000**, 15, 617.

(9) (a) Harvey, P. D.; Sharman, J. G. *Can. J. Chem.* **1990**, 68, 223. (b) Prim, D.; Auffrant, A.; Plyta, Z. F.; Tranchier, J. P.; Rose-Munch, F.; Rose, E. *J. Organomet. Chem.* **2001**, 624, 124. (c) Anson, M.; Polborn, K.; Müller, T. J. *J. Eur. J. Inorg. Chem.* **2000**, 2003. (d) Silverstein, R. M.; Bassler, G. C.; Morrill, T. C. In *Spectrometric Identification of Organic Compounds*, 4th edition; J. Wiley and Sons: New York, 1981; Ch. 3, pp 117–118.

(10) Delavaux, B.; Lepetit, C.; Chermette, H. unpublished results.

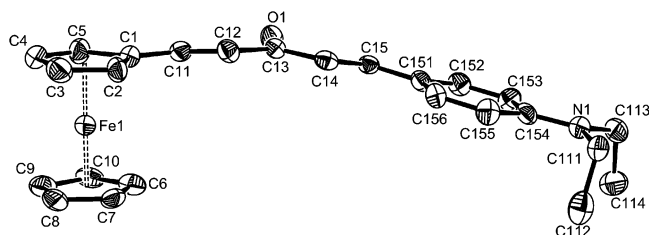


Figure 2. Molecular view of the structure of compound **3** (ORTEP 3) with 50% thermal ellipsoids.

Table 1. Crystallographic Data for Compounds [(C₅H₅)Fe(C₅H₄CO(CH=CH)₂C₆H₄NMe₂)] **2** and [(C₅H₅)Fe(C₅H₄((CH=CH)CO(CH=CH)C₆H₄NEt₂))] **3**^a

	2	3
chemical formula	C ₂₃ H ₂₃ NOFe	C ₂₅ H ₂₇ NOFe
fw	385.27	413.33
cryst syst	monoclinic	monoclinic
space group	P2 ₁ /n	P2 ₁ /a
a, Å	5.7050(10)	9.8308(11)
b, Å	26.841(5)	12.205(2)
c, Å	12.086(2)	16.792(2)
β°	90.55(3)	91.364(15)
V, Å ³	1850.6(6)	2014.2(5)
ρ _{calc} , mg/m ³	1.383	1.363
Z	4	4
μ (mm ⁻¹)	0.826	0.764
T, K	160(2)	180(2)
R ₁ [I > 2σ(I)]	0.0397	0.0488
wR ₂ [I > 2σ(I)]	0.0927	0.0930
R ₁ (all data)	0.0621	0.0946
wR ₂ (all data)	0.1014	0.1058

$$^a R_1 = \sum ||F_o| - |F_c|| / \sum |F_o|; wR_2 = \{ \sum [w(F_o^2 - F_c^2)^2] / \sum [w(F_o^2)^2] \}^{1/2}.$$

Table 2. Selected Bond Lengths (Å) and Angles (deg) for Compounds **2** and **3** with Esd's in Parentheses

bond lengths (Å)		bond angles (deg)	
Compound 2			
C1a–C(1)	1.474(4)	O(1)–C(1)–C(2)	122.0(2)
O(1)–C(1)	1.231(3)	O(1)–C(1)–C(1a)	120.4(2)
C(1)–C(2)	1.472(4)	C(2)–C(3)–C(4)	125.7(3)
C(2)–C(3)	1.339(4)	C(4)–C(5)–C(6)	127.8(3)
C(3)–C(4)	1.441(4)	C(8)–C(7)–C(6)	121.3(3)
C(4)–C(5)	1.343(4)	C(7)–C(8)–C(9)	122.1(3)
C(5)–C(6)	1.454(4)	C(8)–C(9)–N(1)	122.3(3)
C(7)–C(8)	1.384(5)	C(9)–N(1)–C(12)	117.8(4)
C(9)–N(1)	1.385(4)	C(8)–N(1)–C(12)	116.3(3)
N(1)–C(13)	1.445(5)	C(9)–N(1)–C(13)	120.2(3)
Compound 3			
C1–C(11)	1.443(10)	C(1)–C(11)–C(12)	127.7(5)
C(11)–C(12)	1.320(8)	C(11)–C(12)–C(13)	123.4(5)
O(1)–C(13)	1.252(7)	C(12)–C(13)–O(1)	120.8(6)
C(13)–C(14)	1.463(9)	O1–C(13)–C(14)	121.4(6)
C(14)–C(15)	1.327(9)	C(14)–C(15)–C(151)	127.2(5)
C(15)–C(151)	1.454(9)	C(15)–C(151)–C(152)	120.5(5)
C(152)–C(153)	1.374(8)	C(152)–C(153)–C(154)	119.9(7)
C(154)–N(1)	1.384(5)	C(153)–C(154)–N(1)	120.5(6)
N(1)–C(113)	1.440(9)	C(154)–N(1)–C(113)	121.6(5)
N(1)–C(111)	1.459(8)	C(154)–N(1)–C(111)	119.7(6)

moieties,¹¹ as well as the C=O, C₅H₄–C, and C=C distances, compare well with values reported in the literature.^{12,13} For each compound, the olefinic bonds are always cis to the CO function. In both compounds, the organic chain is almost planar. The largest deviation from planarity is

(11) (a) Lindeman, S. V.; Bozak, R. E.; Hicks, R. J.; Husebye, S. *Acta Chem. Scand.* **1997**, *51*, 966. (b) Allen, F. H.; Kennard, O.; Watson, D. G.; Brammer, L.; Orpen, G. A.; Taylor, R. J. *Chem. Soc., Perkin Trans. 2* **1987**, *12*, S1.

located around the C5–C6 bond for **2**; the C4–C5–C6–C7 torsion angle being indeed 20.5°, whereas in compound **3**, the highest observed torsion angle is 11.4° for C11–C12–C13–C14. The organic substituent appears as slightly folded around the CO function: the dihedral angle between the two Cp–CO and CO–Ph average planes is approximately 13.7°. To our knowledge, the unique example of monosubstituted compound presenting a C₅H₄COCH=CHC₆H₄– linkage and structurally characterized is the complex [(C₅H₅)Fe(C₅H₄COCH=CHC₆H₄NO₂)] (**A**).^{11a} This compound is also roughly planar, and the CO and C=C functions are also cis. The observed conformation is the most reasonable for steric reasons. The C–N distances in **2** and **3**, 1.385(4) and 1.384–(5) Å, respectively, are close to the value observed in [(C₅H₅)Fe(C₅H₄COC₆H₄NH₂)]:^{9c} 1.368(9) Å. As expected, these distances are longer than that of **A**: 1.224(11) Å bearing an electron-withdrawing NO₂ function.

The UV–vis spectrum of **1** recorded in CH₃CN exhibits an intense band at 404 nm attributed to a charge transfer (CT) from the donor amino group to the acceptor carbonyl group. The absorption spectra of **2** and **3** exhibit a similar CT band at 412 and 418 nm, respectively. As for compound **1**, these compounds are not fluorescent in this solvent. However, in the solid state, the quasi planarity of the ferrocene substituents is in favor of the existence of a π conjugation that might induce a good electronic communication through the link in solution.

2. Electrochemical Studies. A. Characterization of Compounds 1, 2, and 3. The electrochemical properties of the ligands **1**, **2**, and **3** have been investigated in CH₃CN (Table 3) and typical voltammograms of these species are presented in Figure 3. For compounds **1** and **3** the first wave was observed in cyclic voltammograms (CV) at anodic peak potential (E_{pa}) = 0.70 and 0.60 V, respectively. This is due to the oxidation of the ferrocene moiety and corresponds to a quasi-reversible process whose half wave potential ($E_{1/2}$) value was determined by linear voltammetry. In CV, other irreversible processes observed at more anodic potentials values are attributed to the oxidation of the organic substituent of the molecules. In contrast, the CV of compound **2** exhibits a first peak corresponding to an irreversible oxidation process, followed by the quasi-reversible Fe(II/III) oxidation process calculated at $E_{1/2}$ = 0.72 V. For the three compounds, a single wave was observed in reduction below cathodic peak potential (E_{pc}) = –1.55 V.

Electrochemical cation recognition is mainly based on the variation of the iron (II/III) oxidation potential upon ion addition. To gain a better understanding of the above-described electrochemical processes for **1**, **2**, and **3**, elec-

(12) For CpCOC=C linkage: (a) Shottenberger, H.; Buchmeiser, M. R.; Angleitner, H.; Wurst, K.; Herber, R. H. *J. Organomet. Chem.* **2000**, *605*, 174. (b) Bényei, A. C.; Glidewell, C.; Lightfoot, P.; Royles, B. J. L.; Smith, D. M. *J. Organomet. Chem.* **1997**, *539*, 177. (c) Gyepes, E.; Glowiak, T.; Toma, S. *J. Organomet. Chem.* **1986**, *316*, 163.

(13) For CpC=CCO linkage: (a) Constable, E. C.; Edwards, A. J.; Martinez-Manez, R.; Raithby, P. R. *J. Chem. Soc., Dalton Trans.* **1995**, 3253. (b) Constable, E. C.; Edwards, A. J.; Marcos, M. D.; Raithby, P. R.; Martinez-Manez, R.; Tendero, M. J. L. *Inorg. Chim. Acta* **1994**, *224*, 11. (c) Sato, M.; Mogi, E. *J. Organomet. Chem.* **1996**, *517*, 1.

Table 3. Electrochemical Properties of Compounds **1**, **2**, and **3** in CH₃CN^a

compd	$E_{pa}(\text{Fe})$	$E_{1/2}(P)$	ΔE_p	RI_p	$E_{pa}(\text{Org.})$	$E_{1/2}(P)^b$	$E_{pc}(\text{Red.})$	$E_{1/2}$
1	0.70	0.64 (52)	63	1.0	0.92; 1.60	0.84 (47); 1.50	-1.78	-1.69
2	0.79	0.72 ^c			0.68; 0.98; 1.36		-1.68	-1.52
3	0.60	0.55 (53)	85	1.0	0.87; 1.56	0.82 (49); 1.35	-1.58	-1.48

^a P , ΔE_p (mV); $E_{1/2}$, E_{pa} (V). $\Delta E_p = E_p(\text{forward}) - E_p(\text{backward}) = E_{pa} - E_{pc}$. $RI_p = |I_p(\text{forward})/I_p(\text{backward})| = |I_{pox}/I_{pred}|$. P = slope of the linear regression of $E = f(\log|i/i_d - i|)$. Org. = oxidation processes of the organic part of the molecule. Red. = lone process observed in reduction for the organic part. ^b For the first oxidation process of the organic part. ^c Calculated as the average of anodic (E_{pa}) and cathodic (E_{pc}) peak potentials. Conditions: [complexes], 10^{-3} M; Pt electrode (1 mm diameter); scan rate in cyclic voltammetry, 100 mV s^{-1} ; scan rate in linear voltammetry: 5 mV s^{-1} ; solution of $0.1 \text{ M } ^n\text{Bu}_4\text{NBF}_4$ in CH₃CN; reference electrode SCE.

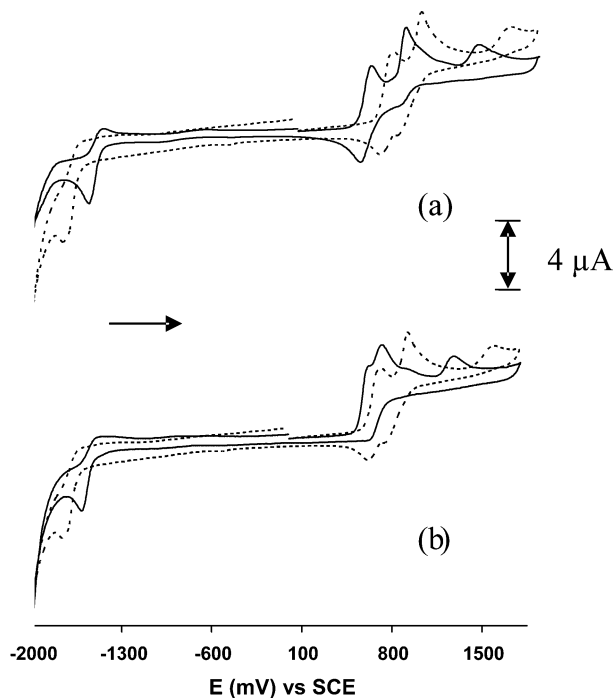


Figure 3. Cyclic voltammograms of (a) compounds **1** (dashed line) and **3** (solid line) and (b) compounds **1** (dashed line) and **2** (solid line). Experimental conditions: Pt electrode (1 mm diameter) in 0.1 M solution of $^n\text{Bu}_4\text{NBF}_4$ in CH₃CN, scan rate 100 mV s^{-1} , ligand concentration 10^{-3} M; reference electrode SCE.

Electrochemical properties of some related iron and organic compounds have been investigated in the same experimental conditions. Among them, the new compounds [(C₅H₅)Fe(C₅H₄-CO(CH=CH)₂C₆H₄NEt₂)] (**7**) and [(C₅H₅)Fe(C₅H₄(CH=CH)₂-CO(CH=CH)C₆H₄NEt₂)] (**8**) were synthesized and characterized as described in the Experimental Section. The results are reported in Table 4, and the following trends appear. (i) Introduction of a -CH=CH- function before the CO group induces a noticeable cathodic shift (ca 100 mV) of the iron oxidation potential ($E_{1/2}$ Fe). (ii) An anodic shift of the organic irreversible reduction process ($E_{1/2}$ Red) occurs simultaneously, and is more important for a double -CH=CH- insertion. This last phenomenon is also observed for the organic compounds. (iii) For the compounds bearing an amino group, an irreversible oxidation process whose $E_{1/2}$ value is found between 0.63 and 1.10 V is observed. This may be attributed to the oxidation potential of the organic amine moiety ($E_{1/2}$ Org) because it lies in the range of values reported for the oxidation of some aza ferrocenyl compounds.⁵

Conjugation of an electron-withdrawing olefinic fragment with a ferrocene moiety has been reported to induce an

anodic shift of the Fe(II)/Fe(III) potential when compared to ferrocene.¹⁴ In contrast, our results are in agreement with previously reported data of related compounds.^{6a} Moreover, as an example, Dowling et al.¹⁵ have shown that insertion of a -CH=CH- group in the Fc-CN bond induced a cathodic shift (210 mV) of the Fe(II)/Fe(III) couple, which can be compared with our findings.

As far as the irreversible reduction process is concerned, it is well-known that when an electroreducible group is conjugated with olefinic groups, the molecule becomes under comparable conditions more easily reducible, as well illustrated by α,β -unsaturated carbonyl.¹⁶ The reduction mechanisms of the α,β -unsaturated carbonyls depends on many factors such as acid-base reactions, preceding, accompanying, and following electron transfer or on the cathode material. The $E_{1/2}$ values (below -1.50 V) found here for the reduction of **1**, **2**, and **3** are therefore attributed to a reduction process mainly located on the CO function. Let us remark that for compound [CH₃COCH=CHC₆H₄NEt₂] the reduction process was absent in CH₂Cl₂, whereas in CH₃CN the use of an Au electrode allowed the clear $E_{1/2}$ determination at -1.84 V .

Studies of the oxidation of organic amines have shown that the primary electrode process for amines is the transfer of an electron from the lone pair of nitrogen to the anode to form a cationic radical.¹⁷ Oxidation of aliphatic amines typically involves the formation of the amine or ammonium salt which arises from hydrogen abstraction from the solvent by the generated radical, whereas radical coupling is favored by aromatic amines.¹⁸ Ferrocenyl aliphatic amines may have the same behavior as their organic counterparts.^{1e,19,20} These results suggest that different and/or competitive mechanisms may be responsible for the second (and third) irreversible organic oxidation wave observed for our compounds. Moreover, it must also be underlined that in these latter cases the spacer between the ferrocene moiety and the organic part is unsaturated, which certainly also affects the oxidation amine response.

- (14) Beer, P. D.; Kocian, O.; Mortimer, R. J. *J. Chem. Soc., Dalton Trans.* **1990**, 3283.
 (15) Dowling, N.; Henry, P. M.; Lewis, N. A.; Taube, H. *Inorg. Chem.* **1981**, *20*, 2345.
 (16) In *Organic Electrochemistry: An Introduction and a Guide*; Baizer, M., Ed.; Marcel Dekker: New York, 1973.
 (17) Ross, S. D.; Finkelstein, M.; Rudd, E. J. *Anodic Oxidation*; Academic Press: New York, 1975; Vol. 32, Ch. 8, p 189.
 (18) (a) Prins, R.; Koorswagen, A. R.; Kortbeek, A. G. T. *J. Organomet. Chem.* **1972**, *39*, 335. (b) Prins, R. *Mol. Phys.* **1970**, *19*, 603.
 (19) (a) Spescha, M.; Duffy, N. W.; Robinson, B. H.; Simpson, J. *Organometallics* **1994**, *13*, 4895.

Table 4. Selected Electrochemical Characteristics of Related Iron or Organic Compounds in CH₃CN^a

compound	$E_{1/2}$ Fe	$E_{1/2}$ Org. (E_{pa})	$E_{1/2}$ Red. (E_{pa})
FcCOMe	0.69	---	---
Fc(CH=CH)CHO	0.58	---	-1.77
Fc(CH=CH)COC ₆ H ₅ ^{6a}	0.56	x ^b	x
Fc(CH=CH)CO(CH=CH)C ₆ H ₅	0.55	---	-1.34
Fc(CH=CH)CO(CH=CH)C ₆ H ₄ NEt ₂ (3)	0.55	0.82	-1.48
Fc(CH=CH) ₂ CO(CH=CH)C ₆ H ₄ NEt ₂ (8)	0.50	0.79	-1.35
FcCO(CH=CH)C ₆ H ₅ ^{6a}	0.69	x	x
FcCO(CH=CH)C ₆ H ₄ NEt ₂ (1)	0.64	0.84	-1.69
FcCO(CH=CH) ₂ C ₆ H ₅	0.68	---	-1.42
FcCO(CH=CH) ₂ C ₆ H ₄ NMe ₂ (2)	0.72 ^e	(0.68)	-1.53
FcCO(CH=CH) ₂ C ₆ H ₄ NEt ₂ (7)	0.74 ^e	(0.66)	-1.58
CH ₃ C ₆ H ₄ NEt ₂ ^c	---	0.71	---
CHOC ₆ H ₄ NEt ₂	---	1.11	---
CHO(CH=CH)C ₆ H ₄ NMe ₂	---	0.85	-1.62
CHO(CH=CH)C ₆ H ₄ NEt ₂	---	0.84	-1.81
CH ₃ CO(CH=CH)C ₆ H ₄ NEt ₂	---	0.78	(-1.89)
C ₆ H ₅ (CH=CH)CO(CH=CH)C ₆ H ₄ NEt ₂	---	0.75	-1.31
CO((CH=CH)C ₆ H ₄ NEt ₂) ₂	---	0.68	-1.48
Fc(CH=CH)C ₆ H ₄ NMe ₂ ⁴³	0.34	0.63	x
Fc(COCH ₂) ₂ CHC ₆ H ₄ NEt ₂ ^{2b}	0.96	0.73	---

^a In our standard conditions. Fc = C₅H₅FeC₅H₄-. Org. = first oxidation process of the organic part. Red. = process observed in reduction for the organic part. ^b x = not mentioned. ^c Quasi-reversible process. ^d --- = not observed. ^e Calculated as the average of anodic (E_{pa}) and cathodic (E_{pc}) peak potentials. For the synthesis of the compounds see Experimental Section.

B. Electrochemical Calcium Detection by Compounds

1, 2, and 3. Electrochemical tests were first performed with **1** (10⁻³M) in acetonitrile in the presence of various cations (Li⁺, Na⁺, K⁺, Ba²⁺, Mg²⁺, Ca²⁺, Cu⁺, Cu²⁺, and Zn²⁺). Complex and particular changes occurred in the presence of the copper cations and are not described here. Compound **1** was poorly sensitive to the presence of cations other than Mg²⁺ and Ca²⁺. In addition, the design of interesting chemosensors which are specific to these latter biologically relevant cations represents a challenging task for many groups.²¹ As the Ca²⁺ electrochemical sensing was very clear for compound **1** we were especially interested in it. Compounds **2** and **3** were also evaluated toward this cation in the same conditions. Addition of 1 equiv of Ca(CF₃SO₃)₂ to compounds **1**, **2**, and **3** induced a clear shift of the Fe(II/III) couple toward anodic potential for **1** and **3** ($\Delta E_{1/2}$ = 58 and 32 mV, respectively) and toward cathodic potential for **2** ($\Delta E_{1/2}$ = -24 mV) (Figure 4).

In cyclic voltammetry, upon calcium addition, the shifted waves corresponding to the iron (II) oxidation processes are still quasi-reversible processes. Simultaneously, the waves corresponding to the oxidation processes of the organic part of the molecule disappeared. The "CO" reduction process becomes poorly defined: an important broadening of the wave accompanied with a variable anodic shift of the reduction potential could be observed. The main reproducible feature observed in reduction for each of compounds **1**, **2**, and **3** was the appearance of a new irreversible process situated at $E_{1/2}$ = -0.16, -0.17, and -0.22 V, respectively, and presenting an important ΔE_p value: 210, 240, and 440 mV, respectively (vide infra). Under our experimental conditions, it was also determined that the reduction of the

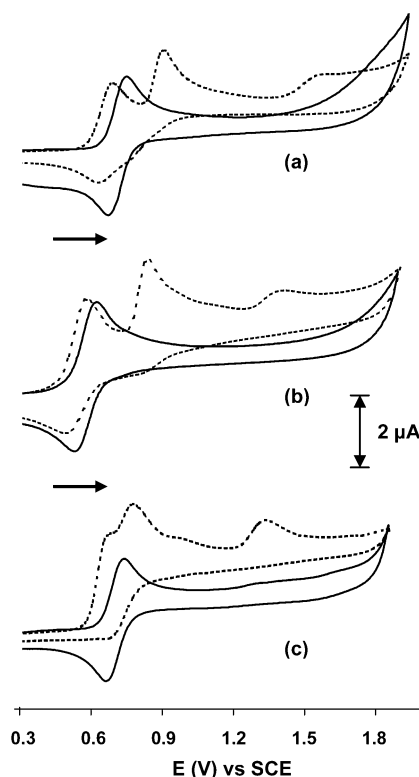


Figure 4. Segmented cyclic voltammograms of compounds (a) **1**, (b) **3**, and (c) **2**, before (dashed lines) and after (solid lines) addition of 1 equiv of Ca(CF₃SO₃)₂. Experimental conditions: Pt electrode (1 mm diameter) in 0.1 M solution of ⁿNBu₄BF₄ in CH₃CN, scan rate 100 mV s⁻¹, ligand concentration 10⁻³ M; reference electrode SCE.

Ca(CF₃SO₃)₂ salt could occur in two principal ranges of potential varying with the salt concentration. For example, the reduction processes observed for 1 equiv (10⁻³ M concentration) were situated at $E_{1/2}$ = -0.09 V (ΔE_p = 349 mV) and -1.03 V (ΔE_p = 539 mV).

Generally, addition of a metal cation induces a classical anodic shift of the iron potential.¹ To our knowledge, only one cathodic iron shift has been reported upon cation addition

(20) Duffy, N. W.; Harper, J.; Ramani, P.; Ranatunge-Bandarage, R.; Robinson, B. H.; Simpson, J. *J. Organomet. Chem.* **1998**, *564*, 125.
 (21) (a) Ajayaghosh, A.; Arunkumar, E.; Daub, J. *Angew. Chem., Int. Ed.* **2002**, *41*, 1766. (b) Chesney, A.; Bryce, M. R.; Batsanov, A. S.; Howard, J. A. K.; Goldenberg, L. M. *Chem. Commun.* **1998**, 677.

Table 5. NMR Shift Variations (Δ (δ), ppm) of Selected Groups of Compounds **1**, **2**, and **3** upon (a) Calcium Addition (1 equiv) and (b) Protonation (1 equiv); [L] = 5×10^{-3} M^a

compd	CHa	CHb	CHc	CHd	N-CH	CHe	CHf	CHg	CHh	CHi	CHj	CO
(a) Calcium Addition												
1 H	-0.01	0.17	0.01	-0.02	0	0.11	0.09					
C	-1.07	2.67	0.71	0.03	0.07	0.68	1.16					2.77
2 H	0.01	0.14	-0.01	-0.02	0	0.09	0.09	0.01	0.03			
C	-0.83	2.18	0.35	0.06	0	0.60	1.06	-0.24	1.60			2.19
3 H	0.06	0.24	0.02	-0.03	0	0.01	0.06			0.07	0.24	
C	-1.02	3.72	1.02	0.11	0.13	0.59	0.93			-0.83	4.24	1.93
(b) Protonation												
1 H	0.31	0.11	0.40	0.82	0.23	0.05	0.10					
C	8.46	-3.50	-0.07	11.62	9.96	0.35	1.01					-0.07
2 H	0.21	-0.01	0.29	0.83	0.35	0.02	0.04	0.31	0.07			
C	4.09	-1.92	0.26	8.93	7.45	0.31	0.74	7.33	-3.66			0.61
3 H ^b	0.48	0.09	0.42	0.81	0.17	0.04	0.05			-0.03	0.18	
C ^b	7.07	-3.68	-0.08	11.75	10.07	0.39	0.77			-0.55	3.59	0.38

^a See group labeling in Scheme 1. H = ¹H NMR {400 MHz}, Δ (δ H) for the proton(s) in CD₃CN at 293K. C = ¹³C NMR {100.6 MHz}, Δ (δ C) for the carbon atom(s) in CD₃CN at 293K. - = Upfield shift. ^b At 233K (see main text).

in CH₃CN (for K⁺, $\Delta E_{1/2} = -30$ mV) and was assigned to an important electronic reorganization of the molecule.²² In case of the ligand **2**, the nature of this uncommon cathodic shift is developed in section 5.

Andrews et al.,⁵ studying the electrochemical properties of the free CO related complex [(C₅H₅)Fe(C₅H₄CH=CHC₆H₄-NMe₂)], bearing an unsaturated link, have shown that the complexation of the Li⁺ cation by the nitrogen atom induced the disappearance of the dialkylamine oxidation wave. This electrochemical behavior is reminiscent of that obtained with compounds **1**, **2**, and **3** in the presence of Ca²⁺ and indicates that such a nitrogen complexation could also occur with compounds **1–3**.

Addition of Li⁺ to ferrocene bis-tertiary amide [Fe(C₅H₄-CONR₂)₂] also resulted in a shift of the ferrocene oxidation wave to more positive potentials (<65 mV).²³ Also when this compound incorporates a nitrogen atom and a CO function, the Li⁺ cation is binding the ligand through carbonyl oxygen donor atoms. In contrast, the monosubstituted compound [(C₅H₅)Fe(C₅H₄CONMe₂)] was insensitive to the presence of this cation. From these studies, it appears that cation interaction with analogues complexes of **1**, **2**, and **3** is not always predictable as illustrated by the versatile electrochemical affinity of the CO function toward Li⁺. These latter examples indicated to us that a Ca²⁺-CO complexation could also occur with compounds **1–3**.

So far, no results have been reported regarding the electrochemical ability of these three literature-cited compounds toward Ca²⁺ addition. However, considering (i) the aboved mentioned results established in refs 5 and 23, and (ii) the changes observed by cyclic voltammetry for our compounds upon calcium addition, it appears that the Ca²⁺ complexation process could involve the whole organic part of these molecules because *both* their oxidation and reduction processes were entirely perturbed. A thorough NMR study was therefore undertaken in order to get further insight into the direct ligand-Ca²⁺ complexation (or interaction) process

itself. The aim of this study was to clarify, as suggested by the electrochemical analysis, that the amine moiety and/or the CO function could be involved in this process, and to quantify this interaction by determining its association constant(s).

3. NMR Study. A. Ca²⁺ Interaction with Compounds **1, **2**, and **3** and their Protonation Reaction.** When treated with 1 equiv of Ca(CF₃SO₃)₂ salt, an orange solution of compound **1** or a red solution of compound **2** or **3** in CH₃CN instantaneously turned deep red. When this mixture was evaporated to dryness and the ¹H NMR spectra of the red residue were recorded in CDCl₃, only the free ferrocenyl ligand L (**1**, **2**, or **3**) was recovered. In contrast, in CD₃CN, NMR spectra were indicative of a ligand-Ca²⁺ interaction. To properly ascertain the variations of the shift observed, 2D NMR (400 MHz, CD₃CN) experiments were performed in a 1:1 ligand/Ca²⁺ ratio. The atom labeling used is indicated in Scheme 1. After analysis, in ¹H NMR spectra (see Table 5 (a) calcium addition), the main feature observed was the clear deshielding of the Hb proton of the olefinic group (0.14–0.24 ppm), whereas the corresponding Ha proton moved only slightly (0.01–0.06 ppm). For compounds **1** and **2** the deshieldings observed for the He and Hf protons are nearly identical, and significantly more important than that observed for compound **3**. Considering now the second olefinic group, in molecule **2** proton Hh was more affected by the interaction than proton Hg. In molecule **3**, Hi and Hj protons presented very close ¹H NMR characteristics when compared with the Ha and Hb protons. Considering now the ¹³C NMR spectra, significant variations were also noticed: for example, the CO group and the olefinic carbon CHb shifted downfield. For the three ligands, the NEt₂ and NMe₂ groups (N-CH protons) were the only groups to be insensitive to the Ca²⁺ addition, showing they were not involved in this interaction. All these features clearly indicated how the unsaturated C₅H₄CO(CH=CH)_n (*n* = 1, 2) or C₅H₄CH=CHCOCH=CH- part of the molecule, including the Cp rings, contributes to the electronic interaction with the cation through the link. The electrostatic attraction between the Ca²⁺ and the negative electron density of the carbonyl group is the key point of this interaction.²⁴

(22) Beer, P. D.; Danks, J. P.; Heseck, D.; McAleer, J. F. *J. Chem. Soc., Chem. Commun.* **1993**, 1735.

(23) Beer, P. D.; Sikanyika, H.; Blackburn, C.; McAleer, J. F. *J. Organomet. Chem.* **1988**, 350, C15.

To investigate the complexation at the nitrogen atom, compounds **1**, **2**, and **3** were then protonated. In CH_3CN , reaction of compounds **1**, **2**, and **3** with $\text{HBF}_4 \cdot \text{Et}_2\text{O}$ in 1:1 stoichiometry turned the solution from orange or red to pink and afforded the protonated species $[\text{1H}][\text{BF}_4]$ (**4**), $[\text{2H}][\text{BF}_4]$ (**5**), and $[\text{3H}][\text{BF}_4]$ (**6**), respectively. The compounds **4–6** were isolated in good yields (78–90%). Their characterization was fully achieved by ^1H and ^{13}C 2D NMR experiments. In the ^1H NMR spectra (CD_3CN , 400 MHz) the protonation reaction has been confirmed by the appearance of a new signal at $\delta = 8.64$, 9.05, and 8.79 ppm, respectively, attributed to the proton of the NH^+ group.^{1e,25a} In molecules **4** and **6**, the NCH_2 -groups appeared at downfield shift position compared with **1** and **3** respectively, as complex multiplets (i.e., $\delta = 3.69$ (dm), 3.62 (dm)), which was consistent with an additive coupling with the acidic proton and the ammonium quaternarization. In the solid state (IR spectrum, KBr), the $\nu(\text{NH}^+)$ elongation vibrations are located in the 3030–3100 cm^{-1} expected range of values.^{1e,2b,25b} Elemental analyses and mass spectra are also in agreement with the proposed formula as described in the Experimental Section.

Considering more specifically Table 5(b) (protonation), several NMR characteristic features appeared. In each case the molecules were totally affected by this event as shown by all ^1H and ^{13}C NMR shift variations. For **3**, the reported data at 233 K are very close to those obtained at 293 K, but the assignment was clearer for some groups. The CHc, CHe, CHf, and CO groups presented the smallest ^{13}C NMR variations. As expected, strong perturbations occurred in the vicinity of the nitrogen site. In ^1H NMR, the phenyl ring was seriously perturbed, the same $\Delta(\delta\text{Hd})$ value of 0.82 (± 0.01) ppm was observed for the three compounds. The NCH protons were shifted downfield (+ 0.17 to 0.35 ppm) but this perturbation was as important as that observed for the Ha proton (0.31 to 0.48 ppm). For both the compounds **2** and **3**, the olefinic group next to the phenyl group is more affected than the other.

To sum up, these results clearly highlight that compounds **1**, **2**, and **3** have similar NMR behaviors toward protonation that strongly contrast with the one observed upon interaction with calcium.

B. Treatment of the NMR Data and Proposition of a Ca^{2+} Interaction Model. To determine the stoichiometry of the calcium adduct(s) and the number of species involved, the interaction process was further studied by ^1H NMR spectroscopy. The chemical shift variations of all the protons of **1**, **2**, and **3** were plotted versus the $\text{Ca}(\text{CF}_3\text{SO}_3)_2$ concentration in CD_3CN . In Figure 5 (points), a similar decreasing effect following the order $\Delta\delta\text{Hb} > \Delta\delta\text{He}$ and

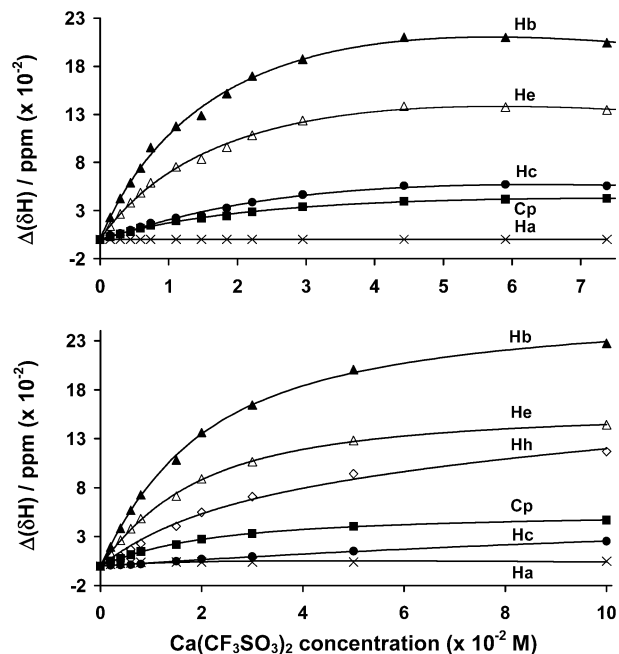


Figure 5. Chemical shift variations of the mentioned protons of **1** (7.4×10^{-3} M) (top), and of **2** (1×10^{-2} M) (bottom), versus the $\text{Ca}(\text{CF}_3\text{SO}_3)_2$ concentration in CD_3CN . See atom labeling in Scheme 1. Experimental values (dots) and calculated (lines) curves obtained by fitting the data.

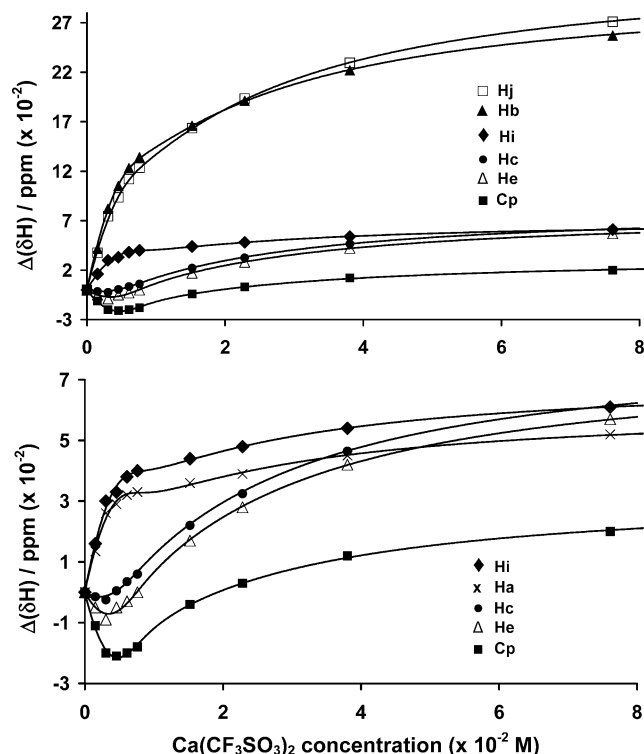


Figure 6. Chemical shift variations of the mentioned protons of **3** (7.6×10^{-3} M) (top) versus the $\text{Ca}(\text{CF}_3\text{SO}_3)_2$ concentration in CD_3CN , and detailed view (bottom) for the Ha, Hi, Hc, He, and Cp protons. See atom labeling in Scheme 1. Experimental values (dots) and calculated (lines) curves obtained by fitting the data.

$\Delta\delta\text{Hf} > (\Delta\delta\text{Hh}) > \Delta\delta\text{Cp} > \Delta\delta\text{Ha}$ is observed for **1** and **2**. The shift variations are often weaker for the other protons and null for the alkyl protons. As provided in Figure 6, in the case of compound **3** the shift variation is rather symmetric with respect to the CO function; see in particular, the couples of curves (Ha, Hi), (Hb, Hj), and (Hc, He).

(24) (a) Ukai, T.; Kawazura, H.; Ishii, Y.; Bonnet, J. J.; Ibers, J. A. *Organomet. Chem.* **1974**, *65*, 253. (b) Marcotte, N.; Fery-Forgues, S.; Lavabre, D.; Marguet, S.; Pivovarenko, V. G. *J. Phys. Chem. A* **1999**, *103*, 3163.

(25) (a) Silverstein, R. M.; Bassler, G. C.; Morrill, T. C. *Spectrometric Identification of Organic Compounds*, 4th ed.; J. Wiley and Sons: New York, 1981; Ch. 3, p 198. (b) Brüggel, H.-J.; Carboo, D.; von Deuten, K.; Knöchel, A.; Kopf, J.; Dreissig, W. *J. Am. Chem. Soc.* **1986**, *108*, 107.

Table 6. Association Constants Related to the LM, L₂M, LM₂, and L₃M Species for Ligands **1**, **2**, and **3** with Calcium in Acetonitrile Determined by Processing the NMR Data^a

compound	LM K ₁ , M ⁻¹	L ₂ M K ₂ , M ⁻¹	LM ₂ K ₃ , M ⁻¹	L ₃ M K ₄ , M ⁻¹
1	11.1	40.9	0	308.0
2	81.0	0	3.8	0
3	3.34 × 10 ³	6.6	40.9	0

^a Values given with ±15% error.

In fact, ligands **1–3** exhibited clear NMR spectra, and a continuous shift of their sharp peaks is observed during the calcium titration experiments. This indicates the presence of fast equilibria on the NMR time-scale. So, for each calcium concentration, only a time-averaged spectrum of the ligand and/or the ligand–calcium complexes is observed. Any observed chemical shift δH_x is, in reality, a mole fraction weighted average of the shifts observed in the free and complexed molecules.

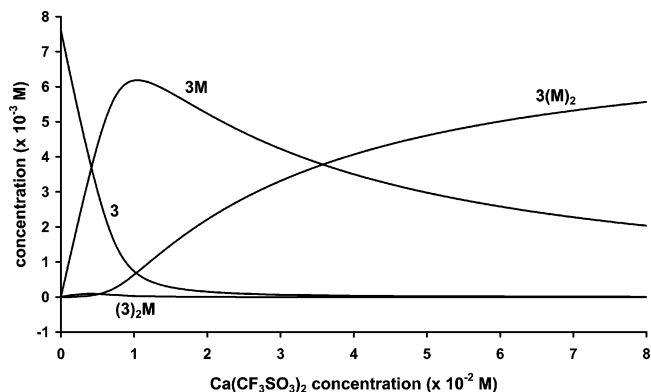
$$\delta H_x = \sum \delta H_x X = \delta H_x^L X_L + \delta H_x^{LM} X_{LM} + 2\delta H_x^{L_2M} X_{L_2M} + \delta H_x^{LM_2} X_{LM_2} + 3\delta H_x^{L_3M} X_{L_3M}$$

where L is the ferrocenyl ligand **1**, **2**, **3**, M is the calcium cation, and X is the mole fraction of the considered species.

The curve-fitting method presents the clear advantage that it can accommodate several L_nM_m complex binding models.²⁶ A previously reported method^{24b,27} was used to determine the association constants for the different L_nM_m complexes present in solution. The following equilibria were considered.



In Figures 5 and 6, the points are experimental and the curves were fitted to the experimental data. Complete fits could not be obtained without taking into account the existence of three species of different stoichiometries for **1** and **3** and of two species of different stoichiometries for compound **2**. The species were for **1**, LM, L₂M, L₃M; for **3**, LM, L₂M, LM₂; and for **2**, LM, LM₂. The corresponding association constants are reported in Table 6. For each ligand the calculated concentrations of the species formed versus calcium concentration indicate that 2M and 3M are formed more quantitatively than 1M but that the LM species is always present in a large Ca²⁺ concentration range (see S5, S6, and Figure 7). Let us remark that LM₂ association constants are quite weaker than those of their LM corresponding species. LM₂ species have already been proposed for related organic

(26) (a) Hynes, M. J. *J. Chem. Soc., Dalton Trans.* **1993**, 311. (b) Fielding, L. *Tetrahedron* **2000**, 56, 6151.(27) Fery-Forgues, S.; Lavabre, D.; Rochal, D. *New J. Chem.* **1988**, 22, 1531.**Figure 7.** Concentration of the formed species versus calcium concentration, [3] = 7.6 × 10⁻³ M.

compounds after treatment of UV–vis data.^{24b} It is noteworthy that substoichiometric compounds L₂M and L₃M are minor species in the case of **1**, and L₂M is present at low concentration (<1 equiv Ca²⁺) for **3**. In the range of concentration considered (7.4 × 10⁻³ to 10⁻² M) for the three compounds several species compete and an example is provided in Figure 7 for compound **3**.

The lack of unique stoichiometry may appear as somewhat troubling and is still uncommon in the literature for ferrocenyl compounds. The existence of several species in equilibrium reflects different possible interactions between the ligand's donor atoms and the Ca²⁺ ion. A screening of the Cambridge data file indicates that the Ca²⁺ may interact with six to nine donor atoms in the case of organic ligand exhibiting the –C=C–C=O linkage, which could account for the presence of substoichiometric compounds of L_nM type where L = **1**, **2**.²⁸ The triflate ion may also interact with the Ca²⁺ ion, thereby increasing the number and nature of possible donor atoms and thus existing interactions, which could help understand the formation of LM_m species.²⁹ However, in the reported equilibria, weak intermolecular interactions (for example with adjacent phenyl group) or electrostatic interactions, rather than classical complexation reactions, may also be considered.

To have experimental proof of the existence of these species from an additional technique, mass spectra were recorded with samples **1**, **2**, and **3** containing 0.5, 1, and 2 equiv of salt, respectively, in the same conditions. The positive FAB technique using an MNBA matrix revealed all the expected peaks for the three compounds (see Experimental Section), confirming thus that strong enough interactions exist between the different ligands and Ca(CF₃SO₃)⁺.

Furthermore, NMR tests performed with **1** in the presence of other cited cations (vide supra) resulted in no (Li⁺) or weak proton shift variations when compared to those due to

(28) For example: (a) Sato, T.; Takeda, H.; Sakai, K.; Tsubomura, T. *Inorg. Chim. Acta* **1996**, 246, 413. (b) Arunasalam, V.-C.; Baxter, I.; Drake, S. R.; Hurtouse, M. B.; Malik, K. M. A.; Miller, S. A. S.; Mingos, D. M. P.; Otway, D. J. *J. Chem. Soc., Dalton Trans.* **1997**, 1331.(29) (a) Lawrance, G. A. *Chem. Rev.* **1986**, 86, 17. (b) Frankland, A. D.; Hitchcock, P. B.; Lappert, M. F.; Lawless, G. A. *J. Chem. Soc., Chem. Commun.* **1994**, 2435. (c) Onoda, A.; Yamada, Y.; Doi, M.; Okamura, T.; Ueyama, N. *Inorg. Chem.* **2001**, 40, 516.

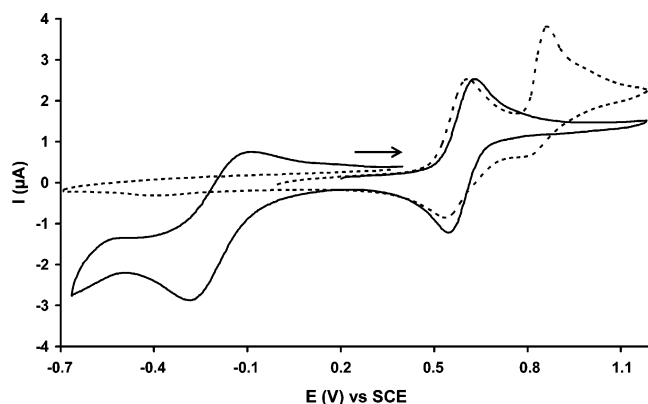


Figure 8. Segmented cyclic voltammograms of compound **3** before (dashed line) and after (solid line) addition of 1 equiv of $\text{HBF}_4 \cdot \text{Et}_2\text{O}$. Experimental conditions: Pt electrode (1 mm diameter) in 0.1 M solution of ${}^n\text{NBu}_4\text{BF}_4$ in CH_3CN , scan rate 100 mV s^{-1} , ligand concentration 10^{-3} M ; reference electrode SCE.

interaction with calcium. In parallel, when an equimolar mixture of Li^+ , Na^+ , K^+ , Ba^{2+} , (4 equiv) in the presence of 1 equiv of Ca^{2+} was added to an acetonitrile electrochemical solution of **1**, the same electrochemical characteristics as induced by Ca^{2+} alone were obtained. These last NMR and electrochemical results are in favor of selectivity for electrochemical detection of Ca^{2+} by **1**. Finally, repeated attempts to isolate calcium–ligand complexes of these receptors in the solid phase were unsuccessful.

4. Electrochemical Properties of the Protonated Compounds 4, 5, and 6. In Section 2, according to electrochemistry studies, both the CO and the amino functions could be suspected to be involved in the detection process. Examination of the ligand– Ca^{2+} interaction has shown in Section 3 that only the CO function was effectively involved in this process. It was then important to study the electrochemical properties of ligands **4**, **5**, and **6** whose the nitrogen sites were protonated.

The electrochemical properties of compounds **4**, **5**, and **6** were investigated under the previously reported conditions. In oxidation, for each compound, the results obtained for the protonated species are similar to those obtained with their corresponding deprotonated forms (**1**, **2**, and **3**) in the presence of one equiv of calcium. In reduction, the currents corresponding to the “CO” reduction processes observed in the range from -1.79 to -1.53 V are weak and cannot be quantified. Passivation phenomena attributed to nonconducting deposits have been observed. The main characteristic feature is the appearance of the new irreversible reduction process around -0.20 V as in the case of calcium addition (vide supra). This last reduction process was attributed to the reduction of the NH^+ function. To verify this hypothesis, the stepwise addition of H^+ (until 1 equiv) to a solution of each compound was also undertaken. In CV, these experiences allowed again the recovery of the same phenomena in oxidation or in reduction. In each case, the final intensity of the wave observed for the NH^+ reduction process was as high as that obtained for the corresponding Fe(II/III) oxidation process, which is in agreement with our attribution. This is illustrated in Figure 8 in the case of compound **3**.

Let us remark, whereas insertion of an olefinic fragment in **1** before the CO function drastically decreases the oxidation potential of the organic part (Figure 3b), this modification induces no change of the oxidation potential of the iron couple in its protonated form $[\text{1H}^+]$: **4** and **5** have approximately the same $E_{1/2}$ value (0.70 V). But, the electronic communication which exists between the nitrogen atom and the ferrocene center decreases as shown by the lowering of the $|\Delta E_{1/2}|$ observed values for **4–6**. Moreover, considering the C1–N1 and C1a–N1 longer than 13 \AA distances in molecules **2** and **3**, the existence of an intramolecular through-space interaction according to Plenio et al.’s model has been ruled out.³⁰

In conclusion, in contrast to NMR studies, when considering Ca^{2+} or H^+ addition, electrochemical measurements gave nearly the same data for the three compounds **1**, **2**, and **3**. To clarify this apparent discrepancy a detailed series of complementary NMR experiments was undertaken.

5. Complementary NMR and Electrochemical Investigations: Link between Calcium Interaction and its Detection? A. NMR Study. At this point, the paramount question is as follows: how could calcium interaction with the ligand and the protonation, involving different molecular sites, lead to the same electrochemical detection? A peculiar role of the electrolyte was suspected. Therefore, the calcium interaction process was first reexamined in the presence of electrolyte. It has been verified that addition of Et_4NBF_4 (or ${}^n\text{Bu}_4\text{NBF}_4$) to an orange solution of compound **1** ($1 \times 10^{-2} \text{ M}$) in 1:1 salt/ligand or 5:1 ratio has no effect (over a 48 h period). Subsequent addition of one equiv of $\text{Ca}(\text{CF}_3\text{SO}_3)_2$ to these solutions turned them red and Ca^{2+} interaction could be observed. After a 4 h period, the solution became pink and the protonated compound $[\text{1H}]^+$ was the unique iron compound detected in solution (see Figure 9). It exhibits a broad downfield shift around 9.2 ppm, which exchanges at low rate (see S7). This signal is sensitive to the presence of other components of the mixture: as small amount of water and CF_3SO_3^- anion. This anion can compete with BF_4^- to yield the $[\text{1H}][\text{CF}_3\text{SO}_3]$ species whose NH^+ shift is 9.5 ppm in CD_3CN (the other NMR shifts are the same than those of **4**).

When the $\text{Ca}(\text{CF}_3\text{SO}_3)_2$ salt was added first to a solution of compound **1** in 1:1 ratio, the ligand interaction was stable over a 48 h period and the solution stayed red. Subsequent addition of Et_4NBF_4 in 1:1 salt/ligand ratio or in 0.2:1 ratio to this mixture led to a pink solution of the protonated compound after 5 and 17 h, respectively.

Compounds **2** and **3** behaved as compound **1**. When 1 equiv of $\text{Ca}(\text{CF}_3\text{SO}_3)_2$ was added to a 1:1 mixture of ligand/ Et_4NBF_4 salt, the red solutions turned deep violet after 4 h. Their respective protonated forms were identified as final and unique iron products.

The triflate supporting electrolyte salt ${}^n\text{Bu}_4\text{NCF}_3\text{SO}_3$ did not react with a solution of compound **1**. In contrast with previous results, subsequent addition of $\text{Ca}(\text{CF}_3\text{SO}_3)_2$ led to

(30) Plenio, H.; Yang, J.; Diodone, R.; Heinze, J. *Inorg. Chem.* **1994**, *33*, 4098.

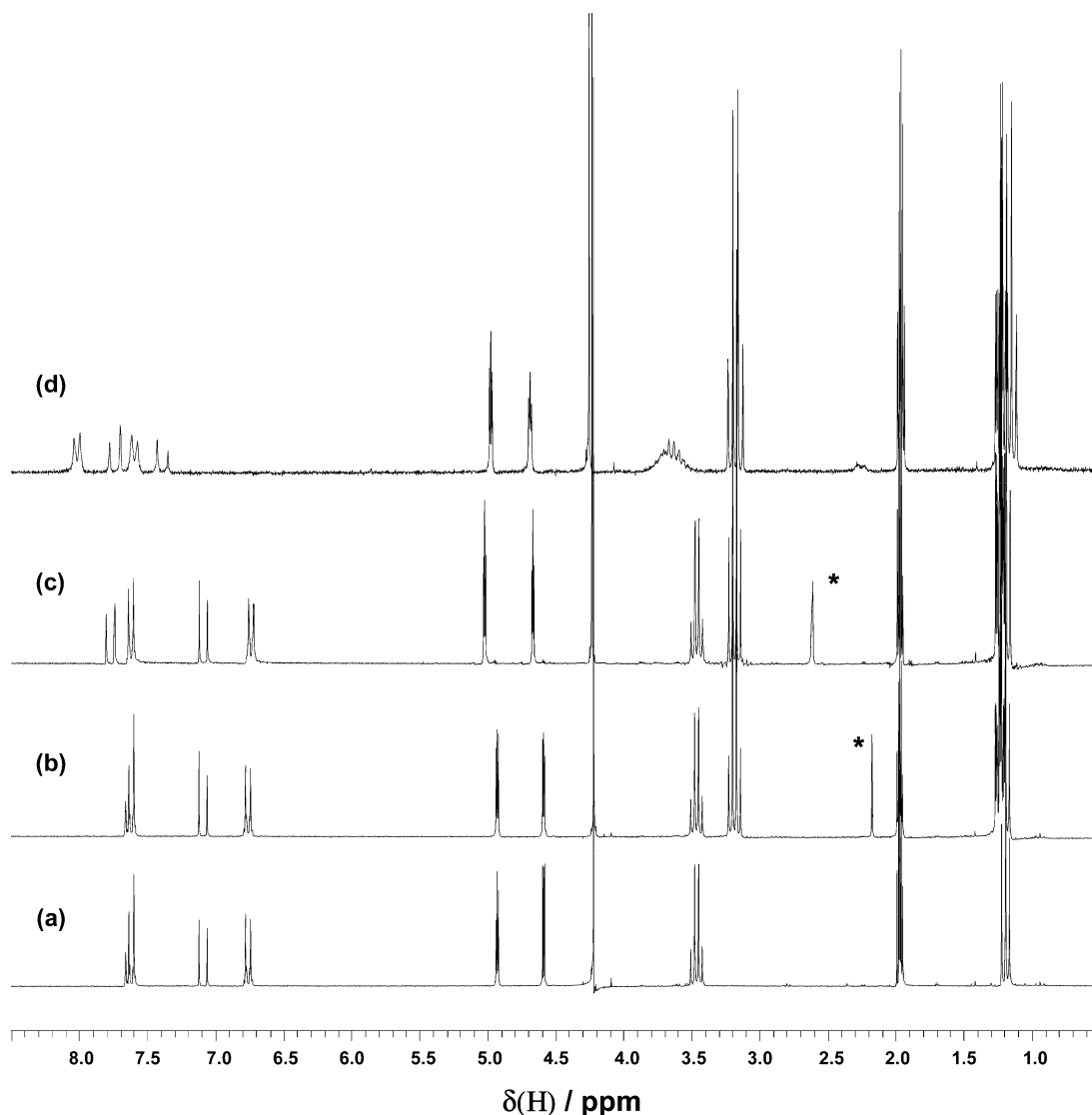


Figure 9. ^1H NMR (250 MHz, CD_3CN) spectra in the 0.5–8.5 ppm range of (a) **1**, (b) **1** + 1 equiv Et_4NBF_4 , (c) mixture (b) + 1 equiv of Ca^{2+} , (d) mixture (c) after 4 h. * H_2O .

the stable red ligand– Ca^{2+} interaction solution over a 24 h period. In this case, no protonation reaction was observed. Consequently, it appears that a small quantity of BF_4^- ion is required to induce a clean protonation of the iron compounds when they interact with Ca^{2+} at NMR concentrations in the presence of ammonium salt. These results clearly highlight why electrochemical detection of $\text{Ca}(\text{CF}_3\text{SO}_3)_2$ may give rise to the same voltammograms as those obtained with the corresponding isolated protonated products or by their in situ protonation.

B. Electrochemical Study. Concerning cation electrochemical detection, competition between complexation and protonation has already been reported but scarcely developed.³¹ In our case, it was important to see whether our NMR conclusions could support electrochemical conditions, especially with an important electrolyte salt/ligand ratio. Detection of the Ca^{2+} cation was reinvestigated by varying the nature of the supporting electrolyte or of the Ca^{2+} compound. As explained earlier, the use of BF_4^- salts (Et_4NBF_4 or $^n\text{Bu}_4\text{NBF}_4$)

allowed $\text{Ca}(\text{CF}_3\text{SO}_3)_2$ electrochemical detection especially by a $\Delta E_{1/2}$ variation of the $\text{Fe}(\text{II})/\text{Fe}(\text{III})$ couple of ≈ 60 mV for compound **1**. Changing the supporting electrolyte by $^n\text{Bu}_4\text{NCF}_3\text{SO}_3$ or $^n\text{Bu}_4\text{NClO}_4$ induced no significant shift of the iron potential; even in Ca^{2+} excess (15 equiv). Water has also been added to the [**1**– Ca^{2+} – $^n\text{Bu}_4\text{NClO}_4$] mixture but no change was observed. Changing now the nature of the calcium salt by using $\text{Ca}(\text{ClO}_4)_2$ but keeping the BF_4^- supporting electrolyte also allowed the same clear detection. This last detection became inefficient if $^n\text{Bu}_4\text{NCF}_3\text{SO}_3$ or $^n\text{Bu}_4\text{NClO}_4$ supporting electrolytes were used.

We have also noticed that clean detection of $\text{Ca}(\text{BF}_4)_2$ was operative whatever the supporting electrolyte used ($^n\text{Bu}_4\text{NBF}_4$ or $^n\text{Bu}_4\text{NCF}_3\text{SO}_3$) and gave the same iron potential shift (60 mV) as in the previously reported conditions. Addition of $\text{Ca}(\text{BF}_4)_2$ to an orange solution of **1** in 1:1 stoichiometry immediately led to a pink solution of the protonated compound **4**. In this case, addition of the supporting electrolyte is not required, probably because of the low

(31) Beer, P. D.; Smith, D. K. *J. Chem. Soc., Dalton Trans.* **1998**, 417.

degree of purity of this calcium salt (70%) when compared to the others.

In conclusion, in the electrochemical conditions the (Ca^{2+} , BF_4^-) couple is required for the formation of the protonated species, which allows the calcium detection. The traces of acid introduced by the ${}^n\text{Bu}_4\text{NCF}_3\text{SO}_3$ electrolyte or the presence of a hydrated perchlorate electrolyte salt are not sufficient to induce this sensing in our standard conditions, contrary to previously reported studies on this topic.³¹

It has already been reported that Ca^{2+} cation can protonate a receptor due to the use of hydrated metal perchlorate salts with ionizable protons.³¹ As shown by NMR and electrochemistry, our ligands are stable in solution in the presence of electrolytes, and their electrochemical characteristics are the same whatever the electrolyte used. Therefore, there is no ligand–electrolyte interaction. The ligand– Ca^{2+} species may interact with the oxygen atom of a water molecule whose one proton becomes more acid. This proton, in the presence of the BF_4^- anion, is then able to protonate the amino part of the ligand, which is not involved in the ligand– Ca^{2+} interaction process. As previously explained (NMR experiment), a sub-stoichiometric amount of BF_4^- electrolyte could be used to induce ligand protonation in the presence of Ca^{2+} salt. Protonation does not occur if the BF_4^- anion is replaced by CF_3SO_3^- or ClO_4^- anion.

How could we now explain the unexpected cathodic shift observed upon calcium addition with ligand **2**? In section 2B, the $E_{1/2}$ shifts observed for ligands **1**, **2**, and **3** upon Ca^{2+} addition correspond, in fact, to those induced by ligands protonation. Thus, for ligands **1** and **3**, the $\Delta E_{1/2}$ of the Fe(II)/Fe(III) couple is positive and represents the difference of the oxidation potential between the protonated form, $[\text{Fe}(\text{II})\text{NH}^+]$ ($E_{1/2} = 0.70$ and 0.57 V), and the neutral form, $[\text{Fe}(\text{II})\text{N}]$ ($E_{1/2} = 0.64$ and 0.54 V), for each compound. In compound **2**, the first oxidation potential of the molecule is attributed to the organic amino moiety, and it precedes now the iron oxidation potential. Consequently, oxidation of **2** first leads to the formation of a cationic radical species: $[\text{Fe}(\text{II})\text{N}^{+\bullet}]$ whose $E_{1/2}(\text{Fe})$ value (0.72 V) is in this case more important than that observed for its corresponding $[\text{Fe}(\text{II})\text{NH}^+]$ form (0.69 V), where the calculated $\Delta E_{1/2}$ is negative, and the observed shift is cathodic. So the unexpected cathodic shift observed for the iron couple of molecule **2** is in connection with its uncommon nature when compared to classical electrochemical ferrocenyl sensors such as **1** and **3**, whose first oxidation potential is due to the iron couple in the protonated and neutral forms.

Concluding Remarks

Noticeable electrochemical Ca^{2+} detection was possible when using new ligands **1**, **2**, and **3** containing a purely organic and original ion sensor subunit with an R-amino complexing moiety ($-\text{COCH}=\text{CHC}_6\text{H}_4-\text{pR}$, $\text{R} = \text{NET}_2$ or NMe_2). This sensing relies on an interaction that occurs between Ca^{2+} and CO moiety of the receptors as demonstrated by a thorough NMR study. This preferred Ca^{2+} interaction could be partially explained in terms of high charge density and oxygen affinity of Ca^{2+} , which induces

thus a stronger interaction than with other tested cations. This interaction gives rise to the formation of several species of different stoichiometries in equilibria, which is uncommon for ferrocenyl compounds. In electrochemistry the detection process is signaled by drastic changes, among them the characteristic shift of the half wave potential of the Fe(II)/Fe(III) couple ($\Delta E_{1/2}$). In parallel, it has also been shown that protonation of **1**, **2**, and **3** arises at the R group and that a through-bond electronic communication along the conjugated chain leads to modifications in cyclic voltammetry similar to those resulting from direct calcium interaction. The combination of different studies led us to the following explanation: Under our standard electrochemical conditions, calcium interaction is followed by protonation and this phenomenon requires the presence of small quantities of BF_4^- anion and of a proton source, probably water. It is noteworthy that the CO function (i) plays a crucial role as coordination site for the interaction, and (ii) does not interrupt the electronic communication between the terminal N donor and the redox ferrocenyl center which could sense the variation of the electronic density. This last remark strengthens the same observation made for organic nonconventional keto spaced chromophores.³² Considering now that protonation is the ultimate step of the Ca^{2+} electrochemical detection, the Ca^{2+} sensing results obtained for **1** and **3** are now clearer. Actually, it has also been reported that through-bond effects are reduced for related compounds that contain a longer conjugated link between the ferrocene center and the binding site.³³ Thus, increasing the distance between the redox center and the complexing site could decrease the $\Delta E_{1/2}$ value. This assumption relies on knowledge of the exact nature of the complexation site and its distance to the redox center. The cathodic shift observed in the case of **2** is in connection with its very nature: the oxidation potential of the initial Fe(II)/Fe(III) couple belongs to a $[\text{Fe}(\text{II})\text{N}^{+\bullet}]$ species and is more important than that of the final protonated form $[\text{Fe}(\text{II})\text{NH}^+]$. We have illustrated in detail, with compounds **1**, **2**, and **3**, how detection or sensing is here not a simple Ca^{2+} molecular interaction or recognition process, as it may occur elsewhere.³⁴ Some elements concerning the pathway from Ca^{2+} interaction to its detection have been clarified. These results also highlight some dependence of this sensing on experimental conditions: a good example is the choice of the different salts used, i.e., reactants and supporting electrolytes. The ligands used are thus capable of detecting the “Ca– BF_4^- ” pair.

Experimental Section

Materials. Toluene was distilled over sodium/benzophenone. Pentane, dichloromethane, and CH_3CN (pure SDS) were distilled over CaH_2 and stored under argon. EtOH analytical grade (purex

(32) Maertens, C.; Detrembleur, C.; Dubois, P.; Jérôme, R.; Boutton, C.; Persoons, A.; Kogej, T.; Bredas, J. L. *Chem. Eur. J.* **1999**, *5*, 369.

(33) (a) Carr, J. D.; Coles, S. J.; Hurthouse, M. B.; Light, M. E.; Munro, E. L.; Tucker, J. H. R.; Westwood, J. *Organometallics* **2000**, *19*, 3312. (b) Chambron, J. C.; Coudret, C.; Sauvage, J. P. *New J. Chem.* **1992**, *16*, 361. (c) Bhadhade, M. M.; Das, A.; Jeffery, J. C.; McCleverty, J. A.; Navas Badiola, J. A.; Ward, M. D. *J. Chem. Soc., Dalton Trans.* **1995**, 2769.

(34) Frabrizzi, L. *Coord. Chem. Rev.* **2000**, *205*, 1.

SDS) was simply degassed. $(C_5H_5)Fe(C_5H_4CHO)$ (98%), $(C_5H_5)Fe(C_5H_4COMe)$ (95%), (Aldrich), $CHOC_6H_4NEt_2$ (99%), $CHOCH=CHC_6H_5$ (98%) (Fluka), $MeCOCH=CHC_6H_5$ (99%), $CHOCH=CHC_6H_4NMe_2$ (98%), $CHOCH=CHC_6H_4NEt_2$ (99%), HBF_4 54% in Et_2O (Aldrich). Calcium salts: $Ca(CF_3SO_3)_2$ (96%) (Strem), $Ca(ClO_4)_2 \cdot 4H_2O$ (99%), $CaBF_4 \cdot xH_2O$ (70%) (Aldrich) were used without purification. Other salts: $LiCF_3SO_3$ (99%) (Strem), $NaCF_3SO_3$ (97%), $Ba(CF_3SO_3)_2$ (97%) (Fluka), KCF_3SO_3 (99%) (Acros), $Zn(CF_3SO_3)_2$ (98%) (Aldrich), $Mg(CF_3SO_3)_2$ (98%) (Fluka). $(C_6H_5-CH=CH)CO(CH=CHC_6H_4NEt_2)$, $MeCOCH=CHC_6H_4NEt_2$, and $CO(CH=CHC_6H_4NEt_2)_2$ were prepared according to the general procedure of Olomucki and Le Gall³⁵ and recrystallized in experimental conditions already described.³⁶ $(C_5H_5)Fe(C_5H_4CH=CHCHO)$ was prepared according a published procedure.³⁷ $(C_5H_5)Fe(C_5H_4CH=CHCOCH=CHC_6H_5)$ was prepared by reaction of $(C_5H_5)Fe(C_5H_4CHO)$ and $MeCOCH=CHC_6H_5$ according to our published procedure.^{2b}

Warning. Perchlorate salts are hazardous because of the possibility of explosion!

General Instrumentation and Procedures. All syntheses were performed under a nitrogen atmosphere using standard Schlenk tube techniques. IR spectra were recorded on a Perkin-Elmer GX FT-IR spectrophotometer. Samples were run as KBr pellets. Elemental analyses were carried out on a Perkin-Elmer 2400 B analyzer at the L. C. C. Microanalytical Laboratory in Toulouse. Mass spectra were obtained at the Service Commun de Spectrométrie de Masse de l'Université Paul Sabatier et du CNRS de Toulouse (fast atom bombardment, FAB^+ ; or desorption chemical ionization, DCI) were performed on a Nermag R 10-10H spectrometer. A 9 kV xenon atom beam was used to desorb samples from the 3-nitrobenzyl alcohol matrix. Other spectra were performed on a triple quadrupole mass spectrometer (Perkin-Elmer Sciex API 365) using electrospray as the ionization mode. The infusion rate was 5 $\mu L/min$. 1H and ^{13}C NMR spectra have been performed on Bruker AC 200, AM 250, DPX 300, and AMX 400 spectrometers. 1H and ^{13}C NMR spectra are referenced to external tetramethylsilane. For 2D NMR experiments, the observation frequencies were in the range 400.13 MHz for 1H and 100.62 MHz for ^{13}C . ($J_{HH} = J_{HCH_2HCH_3}$) for compounds **1**, **2**, and **3**.

Electrochemical Studies. Voltammetric measurements were carried out with a homemade potentiostat³⁸ using the interrupt method to minimize the uncompensated resistance (iR drop). Experiments were performed at room temperature in an airtight three-electrode cell connected to a vacuum/argon line. The reference electrode consisted of a saturated calomel electrode (SCE) separated from the solution by a bridge compartment filled with the same solvent and supporting electrolyte solution. The counter electrode was a platinum wire of ca. 1 cm^2 apparent surface. The working electrode was a Pt electrode (1 mm diameter). The supporting electrolyte nBu_4NBF_4 (99%) (Fluka electrochemical grade), Et_4NBF_4 (99%), or $nBu_4NCF_3SO_3$ (99%) (Aldrich), were melted and dried under vacuum for 1 h, and nBu_4NClO_4 (99%) (Fluka electrochemical grade) was used as received and simply degassed under argon. All solutions measured were 1.0×10^{-3} M in the organometallic complex and 0.1 M in supporting electrolyte. The solutions were degassed by bubbling argon before experiments.

(35) Olomucki, M.; Le Gall, J. Y. *Bull. Soc. Chim. Fr.* **1976**, 9–10, 1467.

(36) Fery-Forgues, S.; Delavaux-Nicot, B.; Lavabre, D.; Rurack, K. J. *Photochem. Photobiol., A* **2003**, 155, 107.

(37) Mongin, C.; Ortin, Y.; Lugan, N.; Mathieu, R. *Eur. J. Inorg. Chem.* **1999**, 5, 739.

(38) Cassoux, P.; Dartiguepeyron, R.; de Montauzon, D.; Tommasino, J. B.; Fabre, P. L. *Actual. Chim.* **1994**, 1, 49.

With the above reference, $E_{1/2} = 0.45$ V vs SCE was obtained for 1 mM ferrocene (estimated experimental uncertainty of ± 10 mV). Cyclic voltammetry was performed in the potential range -2 to 2 V versus SCE scanning from 0 toward 2 V/SCE for oxidation studies (and from 0 toward -2 V/SCE for reduction studies) at 0.1 $V s^{-1}$, at room temperature. Before each measurement, the electrode was polished with Emery paper (Norton A621). To calculate the half wave potential ($E_{1/2}$), the method is as follows: a quasi steady state behavior (at Pt working electrode of 1-mm diameter) is obtained by the use of linear voltammetry at 5 $mV s^{-1}$.

Proton NMR Titration Studies. Proton NMR titrations were typically performed as follows. A solution (500 μL) of the receptor in a deuterated solvent (10^{-2} M) was added (using a microsyringe) into NMR tubes containing the appropriate quantities of solid $Ca(CF_3SO_3)_2$ salt under inert atmosphere, while the NMR spectrum of the receptor was monitored. The samples of solid calcium were prepared by evaporating the corresponding calculated volumes of a calcium guest solution (10^{-2} M) in acetonitrile. Stability constants were evaluated from titration data using the indicated method in the main text.

$[(C_5H_5)Fe(C_5H_4CO(CH=CH)_2C_6H_5)]$. A mixture of $(C_5H_5)Fe(C_5H_4COMe)$ (2.19×10^{-3} mol) and of NaOH (1.1×10^{-2} mol) was solved in ethanol (15 mL). A 300- μL aliquot of $CHOCH=CHC_6H_5$ (2.41×10^{-3} mol) was slowly added to the light-protected stirred solution. The mixture was evaporated to dryness and the residue was dissolved in CH_2Cl_2 (40 mL). The solution was filtered. After evaporation, the product was washed with pentane (50 mL $\times 2$). The red-violet powder was dried under vacuum and obtained in 78% yield. MS-FAB: 342 $[M]^+$. Anal. Calcd for **1**, $C_{21}H_{18}OF_6$: C, 73.71; H, 5.30; N, Found: C, 73.52; H, 5.18. 1H NMR (300 MHz, $CDCl_3$, 298 K): δ 4.23 (s, 5 H, C_5H_5); (4.59, 4.89) (each t, 2 H, $^3J = 2.1$ Hz, C_5H_4); 6.72 (d, 1 H, $^3J = 15.0$ Hz, CH); 7.03 (m, 2 H, C_6H_5); 7.37 (m, 3 H, C_6H_5 , CH); 7.58 (m, 3 H, C_6H_5 , CH).

Syntheses of Ferrocenyl Compounds 1, 2, and 3. In a typical procedure, a mixture of the appropriate reactants in 1:1 stoichiometry (10^{-3} M) and 5 equiv of NaOH was dissolved in ethanol (30 mL) and stirred for 20 h for **1** and **2**, or 5 h for **3**, at room temperature. The mixture was evaporated to dryness and the residue was dissolved in dichloromethane (50 mL). The solution was filtered off and evaporated to dryness. The product was purified by column chromatography on alumina (eluent: pentane/ CH_2Cl_2). After evaporation of the solvent, the product was washed with pentane (50 \times 2 mL) and dried for several hours to afford the desired products as deep orange, red-violet, and violet powders, respectively. Compounds **1**, **2**, and **3** were obtained in 82, 77, and 72% yield, respectively.

$[(C_5H_5)Fe(C_5H_4COCH=CHC_6H_4NEt_2)]$ (1**).** 1H NMR (400 MHz, CD_3CN , 293 K): δ 1.19 (t, 6 H, $^3J_{HH} = 6.8$ Hz, CH_3), 3.46 (q, 4 H, $^3J_{HH} = 6.8$ Hz, CH_2), 4.22 (s, 5 H, C_5H_5), 4.59 (t, 2 H, $^3J_{HeHf} = 1.6$ Hz, Hf), 4.93 (t, 2 H, $^3J_{HeHf} = 1.6$ Hz, He), 6.76 (d, 2H, $^3J_{HcHd} = 8.8$ Hz, Hd), 7.09 (d, 1 H, $^3J_{HaHb} = 15.2$ Hz, Ha), 7.62 (d, 2 H, $^3J_{HcHd} = 8.8$ Hz, Hc), 7.63 (d, 1 H, $^3J_{HaHb} = 15.2$ Hz, Hb). $^{13}C\{^1H\}$ NMR (100.6 MHz, CD_3CN , 293 K): δ 12.25 (s, CH_3), 44.51 (s, CH_2), 69.76 (s, CHf), 70.19 (s, C_5H_5), 72.56 (s, CHf), 82.09 (s, $C_{ipso-C_5H_4}$), 111.69 (s, CHd), 118.06 (s, CHa), 122.11 (s, C_{ipso-C}), 130.84 (s, CHc), 141.24 (s, CHb), 149.84 (s, C_{ipso-N}), 192.52 (s, CO). MS-DCI: 388 $[M + H]^+$. Anal. Calcd for **1**, $C_{23}H_{25}NOFe$: C, 71.33; H, 6.51; N, 3.62. Found: C, 71.26; H, 6.60; N, 3.53.

$[(C_5H_5)Fe(C_5H_4CO(CH=CH)_2C_6H_4NMe_2)]$ (2**).** 1H NMR (400 MHz, CD_3CN , 293 K): δ 3.01 (s, 6 H, CH_3), 4.22 (s, 5 H, C_5H_5), 4.60 (t, 2 H, $^3J_{HeHf} = 1.1$ Hz, Hf), 4.85 (t, 2 H, $^3J_{HeHf} = 1.1$ Hz,

He), 6.77 (d, 2H, $^3J_{\text{HcHd}} = 9.0$ Hz, Hd), 6.78 (dd, 1 H, $^3J_{\text{HaHb}} = 15.4$ Hz, $^4J_{\text{HaHg}} = 0.6$ Hz, Ha), 6.94 (ddd, 1 H, $^3J_{\text{HgHh}} = 15.4$ Hz, $^3J_{\text{HgHb}} = 10.6$ Hz, $^4J_{\text{HaHg}} = 0.6$ Hz, Hg), 7.03 (d, 1 H, $^3J_{\text{HgHh}} = 15.4$ Hz, Hh), 7.45 (dd, 2 H, $^3J_{\text{HcHd}} = 9.0$ Hz, $^4J_{\text{HhHc}} = 0.6$ Hz, Hc), 7.47 (dd, 1 H, $^3J_{\text{HaHb}} = 15.4$ Hz, $^3J_{\text{HbHg}} = 10.6$ Hz, Hb). $^{13}\text{C}\{^1\text{H}\}$ NMR (100.6 MHz, CD_3CN , 293 K): δ 39.83 (s, CH_3), 69.73 (s, CHe), 70.25 (s, C_5H_5), 72.76 (s, CHf), 81.79 (s, $\text{C}_{\text{ipso}}\text{C}_5\text{H}_4$), 112.54 (s, CHd), 122.85 (s, CHg), 124.72 (s, $\text{C}_{\text{ipso}}\text{-C}$), 124.91 (s, CHa), 128.91 (s, CHc), 141.72 (s, CHb), 141.86 (s, CHh), 151.65 (s, $\text{C}_{\text{ipso}}\text{-N}$), 192.73 (s, CO). MS-DCI: 386 [M + H]⁺. Anal. Calcd for **2**, $\text{C}_{23}\text{H}_{23}\text{NOFe}$: C, 71.63; H, 5.97; N, 3.63. Found: C, 71.47; H, 5.63; N, 3.58.

[(C₅H₅)Fe(C₅H₄CH=CHCOCH=CHC₆H₄NEt₂)] (3). ^1H NMR (400 MHz, CD_3CN , 293 K): δ 1.18 (t, 6 H, $^3J_{\text{HH}} = 7.0$ Hz, CH_3), 3.45 (q, 4 H, $^3J_{\text{HH}} = 7.0$ Hz, CH_2), 4.20 (s, 5 H, C_5H_5), 4.50 (t, 2 H, $^3J_{\text{HeHf}} = 1.8$ Hz, Hf), 4.67 (t, 2 H, $^3J_{\text{HeHf}} = 1.8$ Hz, He), 6.75 (d, 2H, $^3J_{\text{HcHd}} = 8.5$ Hz, Hd), 6.78 (d, 1 H, $^3J_{\text{HHj}} = 15.7$ Hz, Hi), 6.90 (d, 1 H, $^3J_{\text{HaHb}} = 15.8$ Hz, Ha), 7.55 (d, 2 H, $^3J_{\text{HcHd}} = 8.5$ Hz, Hc), 7.60 (d, 1 H, $^3J_{\text{HHj}} = 15.7$ Hz, Hj), 7.62 (d, 1 H, $^3J_{\text{HaHb}} = 15.8$ Hz, CHb). $^{13}\text{C}\{^1\text{H}\}$ NMR (100.6 MHz, CD_3CN , 293 K): δ 12.24 (s, CH_3), 44.52 (s, CH_2), 69.17 (s, CHe), 70.00 (s, C_5H_5), 71.38 (s, CHf), 80.21 (s, $\text{C}_{\text{ipso}}\text{C}_5\text{H}_4$), 111.73 (s, CHd), 120.40 (s, CHa), 122.01 (s, $\text{C}_{\text{ipso}}\text{-C}$), 124.03 (s, CHi), 130.79 (s, CHc), 143.13 (s, CHb), 143.33 (s, CHj), 150.00 (s, $\text{C}_{\text{ipso}}\text{-N}$), 187.59 (s, CO). MS-DCI: 414 [M + H]⁺. Anal. Calcd for **3**, $\text{C}_{25}\text{H}_{27}\text{NOFe}$: C, 72.65; H, 6.58; N, 3.39. Found: C, 72.58; H, 6.48; N, 3.27.

Synthesis of [Tetrafluoroborate (1-)] Compounds of 1, 2, and 3: 4, 5 and 6. $\text{HBF}_4\cdot\text{Et}_2\text{O}$ (1 equiv) was slowly syringed into a stirred solution of **1** or **2** or **3** (4×10^{-4} M) in acetonitrile (15 mL). The light-protected mixture solution was stirred for 4 h. After solvent evaporation, the product was washed with ether (30 mL) and pentane (40 mL) and dried under vacuum. A violet powder was obtained in 90, 85, and 72% yield, respectively.

[(C₅H₅)Fe(C₅H₄COCH=CHC₆H₄NHEt₂)](BF₄) (4). ^1H NMR (400 MHz, CD_3CN , 293 K): δ 1.15 (t, 6 H, $^3J_{\text{HH}} = 7.2$ Hz, CH_3), 3.69 (md, 4 H, $^3J_{\text{HH}} = 7.2$ Hz, CH_2), 4.25 (s, 5 H, C_5H_5), 4.69 (t, 2 H, $^3J_{\text{HeHf}} = 1.7$ Hz, Hf), 4.98 (t, 2 H, $^3J_{\text{HeHf}} = 1.7$ Hz, He), 7.40 (d, 1 H, $^3J_{\text{HaHb}} = 15.7$ Hz, CHa), 7.58 (d large, 2 H, $^3J_{\text{HcHd}} = 7.9$ Hz, Hd), 7.74 (d, 1 H, $^3J_{\text{HaHb}} = 15.7$ Hz, Hb), 8.02 (d, 2 H, $^3J_{\text{HcHd}} = 7.9$ Hz, Hc), 8.64 (s large, 1 H, N⁺H). $^{13}\text{C}\{^1\text{H}\}$ NMR (100.6 MHz, CD_3CN , 293 K): δ 10.18 (s, CH_3), 54.74 (s, CH_2), 70.11 (s, CHe), 70.46 (s, C_5H_5), 73.57 (s, CHf), 81.07 (s, $\text{C}_{\text{ipso}}\text{C}_5\text{H}_4$), 123.31 (s, CHd), 126.52 (s, CHa), 130.77 (s, CHc), 137.74 (s, CHb), 138.00 (s, $\text{C}_{\text{ipso}}\text{-N}$), 138.19 (s, $\text{C}_{\text{ipso}}\text{-C}$), 192.45 (s, CO). (KBr, ν , cm^{-1}): 3079, 3029 (ν , NH⁺). MS-DCI: 388 [M - BF₄]⁺. Anal. Calcd for **4**, $\text{C}_{23}\text{H}_{26}\text{NOFeBF}_4$: C, 58.14; H, 5.52; N, 2.95. Found: C, 58.19; H, 5.26; N, 2.90.

[(C₅H₅)Fe(C₅H₄CO(CH=CH)₂C₆H₄NHMe₂)](BF₄) (5). ^1H NMR (400 MHz, CD_3CN , 293 K): δ 3.28 (s, 6 H, CH_3), 4.22 (s, 5 H, C_5H_5), 4.64 (t, 2 H, $^3J_{\text{HeHf}} = 1.6$ Hz, Hf), 4.87 (t, 2 H, $^3J_{\text{HeHf}} = 1.6$ Hz, He), 6.99 (d, 1 H, $^3J_{\text{HaHb}} = 14.8$ Hz, Ha), 7.10 (broad d, 1 H, $^3J_{\text{HgHh}} = 15.6$ Hz, CHh), 7.25 (dd, 1 H, $^3J_{\text{HgHh}} = 15.6$ Hz, $^3J_{\text{HbHg}} = 10.9$ Hz, Hg), 7.46 (dd, 1 H, $^3J_{\text{HaHb}} = 14.8$ Hz, $^3J_{\text{HgHh}} = 10.9$ Hz, Hb), 7.60 (d, 2H, $^3J_{\text{HcHd}} = 8.7$ Hz, Hd), 7.74 (d, 2 H, $^3J_{\text{HcHd}} = 8.7$ Hz, Hc), 9.05 (s large, 1 H, NH⁺). $^{13}\text{C}\{^1\text{H}\}$ NMR (100.6 MHz, CD_3CN , 293 K): δ 47.28 (s, CH_3), 70.04 (s, CHe), 70.48 (s, C_5H_5), 73.50 (s, CHf), 81.42 (s, $\text{C}_{\text{ipso}}\text{C}_5\text{H}_4$), 121.47 (s, CHd), 129.00 (s, CHa), 129.17 (s, CHc), 130.18 (s, CHg), 138.20 (s, CHh), 138.84 (s, $\text{C}_{\text{ipso}}\text{-C}$), 139.80 (s, CHb), 142.42 (s, $\text{C}_{\text{ipso}}\text{-N}$), 193.34 (s, CO). (KBr, ν , cm^{-1}): 3095, 3033 (ν , NH⁺). MS-DCI: 386 [M - BF₄]⁺. Anal. Calcd for **5**, $\text{C}_{23}\text{H}_{24}\text{NOFeBF}_4$: C, 58.39; H, 5.11; N, 2.96. Found: C, 58.37; H, 4.81; N, 3.08.

[(C₅H₅)Fe(C₅H₄CH=CHCOCH=CHC₆H₄NHEt₂)](BF₄) (6). ^1H NMR (400 MHz, CD_3CN , 233 K): δ 1.06 (t, 6 H, $^3J_{\text{HH}} = 7.0$ Hz, CH_3), 3.62 (md, 4 H, $^3J_{\text{HH}} = 7.0$ Hz, CH_2), 4.20 (s, 5 H, C_5H_5), 4.55 (s large, 2 H, Hf), 4.71 (s large, 2 H, He), 6.75 (d, 1H, $^3J_{\text{HHj}} = 15.9$ Hz, Hi), 7.38 (d, 1 H, $^3J_{\text{HaHb}} = 15.9$ Hz, Ha), 7.56 (d, 2 H, $^3J_{\text{HH}} = 8.5$ Hz, Hd), 7.71 (d, 1 H, $^3J_{\text{HaHb}} = 15.9$ Hz, Hb), 7.78 (d, 1 H, $^3J_{\text{HHj}} = 15.9$ Hz, Hj), 7.97 (d, 2 H, $^3J_{\text{HcHd}} = 8.5$ Hz, Hc), 8.79 (s large, 1 H, N⁺H). $^{13}\text{C}\{^1\text{H}\}$ NMR (100.6 MHz, CD_3CN , 233 K): δ 10.35 (s, CH_3), 54.59 (s, CH_2), 69.56 (s, CHe), 70.23 (s, C_5H_5), 72.15 (s, CHf), 79.37 (s, $\text{C}_{\text{ipso}}\text{C}_5\text{H}_4$), 123.48 (s, CHi), 123.48 (s, CHd), 127.47 (s, CHa), 130.71 (s, CHc), 137.78 (s, $\text{C}_{\text{ipso}}\text{-N}$), 137.86 (s, $\text{C}_{\text{ipso}}\text{-C}$), 139.45 (s, CHb), 146.92 (s, CHj), 187.97 (s, CO). (KBr, ν , cm^{-1}): 3106, 3055, (ν , NH⁺). MS-FAB: 414 [M - BF₄]⁺. Anal. Calcd for **6**, $\text{C}_{25}\text{H}_{28}\text{NOFe BF}_4$: C, 59.92; H, 5.63; N, 2.79. Found: C, 59.84; H, 5.58; N, 2.71.

Mass Spectrometry: Interaction of Compounds 1, 2, and 3 with Ca²⁺. The samples were prepared as for the NMR titrations.

For Compound 1. [1M-CF₃SO₃⁻] = 576, [(1)₂M-CF₃SO₃⁻] = 963, [(1)₃M-CF₃SO₃⁻] = 1350.

For Compound 2. [2M-CF₃SO₃⁻] = 574, [(2)₂M₂-HCF₃SO₃]⁺ = 911, [(2)₂M₂]⁺ = 1061.

For Compound 3. [3M-CF₃SO₃⁻] = 602, [(3)₂M-CF₃SO₃⁻] = 1015, [(3)₂M₂-HCF₃SO₃]⁺ = 939, [(3)₂M₂]⁺ = 1089.

[(C₅H₅)Fe(C₅H₄CO(CH=CH)₂C₆H₄NEt₂)] (7). This compound was prepared by the same procedure as previous compounds with FeCOME ($1.48 \cdot 10^{-3}$ mol) and CHOCH=CHC₆H₄NEt₂ as reactants in 1:1 stoichiometry and isolated in 92% yield. ^1H NMR (250 MHz, CD_3CN , 297 K): δ 1.18 (t, 6 H, $^3J_{\text{HH}} = 7.0$ Hz, CH_3); 3.44 (q, 4 H, $^3J_{\text{HH}} = 7.0$ Hz, CH_2); 4.22 (s, 5 H, C_5H_5); (4.59, 4.85) (each t, 2 H, $^3J_{\text{HH}} = 2.1$ Hz, C_5H_4); (6.73, 7.41) (each d, 2H, $^3J_{\text{HH}} = 9.0$ Hz, C_6H_4); (6.77, 7.02) (each d, 1 H, $^3J_{\text{HH}} = 15.3$ Hz, CH); (6.91, 7.47) (each dd, 1 H, $^3J_{\text{HH}} = 15.3$ Hz, $^3J_{\text{HH}} = 10.4$ Hz, CH). $^{13}\text{C}\{^1\text{H}\}$ NMR (75.5 MHz, CD_3CN , 298 K): δ 12.27 (s, CH_3); 44.45 (s, CH_2); (69.71, 72.69) (each s, C_5H_4); 70.23 (s, C_5H_5); 81.86 (s, $\text{C}_{\text{ipso}}\text{C}_5\text{H}_4$); (111.92, 129.24) (each s, C_6H_4); 123.82 (s, $\text{C}_{\text{ipso}}\text{-C}$); 148.98 (s, $\text{C}_{\text{ipso}}\text{-N}$); (122.24, 124.54, 141.87, 142.00) (each s, CH); 192.66 (s, CO). MS-FAB: 413 [M - H]⁺. Anal. Calcd for **7**, $\text{C}_{25}\text{H}_{27}\text{NOFe}$: C, 72.65; H, 6.58; N, 3.39. Found: C, 72.60; H, 6.62; N, 3.31.

[(C₅H₅)Fe(C₅H₄(CH=CH)₂CO(CH=CH)₂C₆H₄NEt₂)] (8). A mixture of (C₅H₅)Fe(C₅H₄CH=CHCHO), MeCOCH=CHC₆H₄NEt₂, and NaOH in 1:1:1 stoichiometry ($6.25 \cdot 10^{-3}$ M) was dissolved in ethanol (10 mL) and stirred for 24 h at room temperature. The mixture was evaporated to dryness and the residue was dissolved in dichloromethane (40 mL). The solution was filtered off and evaporated to dryness. The residue was washed with pentane (2×50 mL) and the product was extracted with hexane to afford a red-violet powder in 69% yield. ^1H NMR (300 MHz, CDCl_3 , 298 K): δ 1.22 (t, 6 H, $^3J_{\text{HH}} = 6.9$ Hz, CH_3); 3.43 (q, 4 H, $^3J_{\text{HH}} = 6.9$ Hz, CH_2); 4.16 (s, 5 H, C_5H_5); (4.39, 4.49) (each t, 2 H, $^3J_{\text{HH}} = 1.8$ Hz, C_5H_4); 6.54 (d, 1 H, $^3J_{\text{HH}} = 15.5$ Hz, CH); 6.58 (dd, 1 H, $^3J_{\text{HH}} = 15.0$ Hz, $^3J_{\text{HH}} = 11.1$ Hz, CH); (6.67, 7.49) (each d, 2 H, $^3J_{\text{HH}} = 8.7$ Hz, C_6H_4); (6.79, 7.68) (each d, 1 H, $^3J_{\text{HH}} = 15.5$ Hz, CH); 6.83 (d, 1 H, $^3J_{\text{HH}} = 15.0$ Hz, CH); 7.42 (dd, 1 H, $^3J_{\text{HH}} = 15.5$ Hz, $^3J_{\text{HH}} = 11.1$ Hz, CH). $^{13}\text{C}\{^1\text{H}\}$ NMR (100.6 MHz, CDCl_3 , 293 K): δ 13.03 (s, CH_3); 44.93 (s, CH_2); (68.16, 70.69) (each s, C_5H_4); 70.00 (s, C_5H_5); 81.83 (s, $\text{C}_{\text{ipso}}\text{C}_5\text{H}_4$); (111.65, 130.97) (each s, C_6H_4); (121.06, 125.24, 127.10, 143.11, 141.71, 143.94) (each s, CH); 122.20 (s, $\text{C}_{\text{ipso}}\text{-C}$); 149.88 (s, $\text{C}_{\text{ipso}}\text{-N}$); 189.55 (s, CO). MS-DCI: 440 [M + H]⁺. Anal. Calcd for **8**, $\text{C}_{27}\text{H}_{29}\text{NOFe}$: C, 73.81; H, 6.65; N, 3.19. Found: C, 73.99; H, 6.56; N, 3.12.

Crystallographic Study of Compounds 2 and 3. For these two compounds data were collected at low-temperature T (180 K) on a

Stoe imaging plate diffraction system (IPDS), equipped with an Oxford Cryosystems cryostream cooler device and using a graphite-monochromated Mo K α radiation ($\lambda = 0.71073 \text{ \AA}$). Final unit cell parameters were obtained by means of a least-squares refinement of a set of 8000 reflections. Crystal decay was monitored in the course of data collection by measuring 200 reflections by image. No significant fluctuations of intensities were observed during measurements. Concerning compound **3** the crystal was found to be twinned. However, the two domains could be indexed and the two orientation matrixes were used in the integration process (STOE, 1996) to produce a set of nonoverlapped reflections for each domain. Only the data from the domain with the strongest intensities were considered. The rejection of all overlapped reflections resulted in a very poor completeness around 57%. Structures were solved by means of direct methods using the program SIR 92³⁹ and subsequent difference Fourier maps. The models were refined by least-squares procedures on a F² using SHELXL-97.⁴⁰ Atomic scattering factors were taken from International Tables for X-ray Crystallography.⁴¹ All hydrogen atoms were located on

difference Fourier maps, but introduced in the refinement as fixed contributors by using a riding model and with an isotropic thermal parameter fixed at 20% (or 50% for CH₃ group) higher than those of the carbon atoms to which they were connected. For the two structures, all non-hydrogen atoms were anisotropically refined, and in the last cycles of refinement weighting schemes were used, where weights were calculated from the following formula: $w = 1/[\sigma^2-(Fo^2) + (aP)^2 + bP]$ where $P = (Fo^2 + 2Fc^2)/3$. Drawings of molecules were plotted using the program ORTEP 3⁴² with 50% probability displacement ellipsoids for non-hydrogen atoms.

Acknowledgment. We are thankful to Professor Dr. Paul-Louis Fabre (Toulouse) for fruitful discussion. We gratefully acknowledge the reviewers for constructive remarks.

Supporting Information Available: Figures S1–S4 giving the compared NMR spectra of compound **L** (**L** = **1**, **2**, and **3**) with 1 equiv of Ca²⁺ and H⁺, respectively. Figures S5 and S6 presenting concentrations of the formed species versus the calcium concentration for ligands **1** and **2**, respectively. Figure S7 giving the compared spectra of compound **4** and of mixture from Figure 9d in the 1–9.5 ppm range. S8 and S9 presenting crystal data of complexes **2** and **3**, and one X-ray crystallographic file, in CIF format. Figures S10 and S11 showing overhead view of molecules **2** and **3**, respectively. S12, NMR data, interaction of compounds **1**, **2**, and **3** with Ca²⁺. This material is available free of charge via the Internet at <http://pubs.acs.org>.

- (39) Altomare, A.; Cascarano, G.; Giacovazzo, G.; Guagliardi, A. SIR92-A program for crystal structure solution. *J. Appl. Crystallogr.* **1993**, *26*, 343.
- (40) Sheldrick, G. M. SHELXL-97, *Program for the Refinement of Crystal Structures*; Institut für Anorganische Chemie der Universität, Tammanstrasse 4, D-3400, Göttingen, Germany, 1997.
- (41) International Tables for X-ray Crystallography, Vol IV; Kynoch Press: Birmingham, England, 1974.
- (42) Farrugia, L. J. ORTEP3 for Windows. *J. Appl. Crystallogr.* **1997**, *30*, 565.
- (43) Beer, P. D.; Blackburn, C.; McAleer, J. F.; Sikanyika, H. *Inorg. Chem.* **1990**, *29*, 378.

IC0345828